Charmless nonleptonic rare decays of B mesons

Ling-Lie Chau
Physics Department, University of California at Davis, Davis, California 95616

Hai-Yang Cheng, W. K. Sze, and Herng Yao*
Institute of Physics, Academia Sinica, Taipei, Taiwan 11529

Benjamin Tseng
Physics Department, National Cheng Kung University, Tainan, Taiwan 70101
(Received 30 July 1990)

Branching ratios of nonleptonic exclusive two-body decays of B mesons without final-state charm particles are studied in detail. The technique used for evaluating the nonleptonic decay amplitudes is elucidated. The dominant charmless decay channels are $B_u^+ \to K^+\eta'$, $\pi^+\eta', \rho^+\pi^0$, $\rho^+\eta, \rho^+\eta'$, $\rho^+\omega, B_d^0 \to K^0\eta', \eta\eta', \eta'\eta', K^{*+}\pi^-, \rho^+\pi^-, K^{*+}\rho^-$, $\rho^+\rho^-$, which should be interesting for experimental observation. The implications of the quark-diagram scheme are also discussed.

I. INTRODUCTION

Although no evidence for purely hadronic $b \to u$ or loop-induced $b \to s$ transitions has been observed, the nonleptonic rare B decays without charm particles in the final state have elicited more and more attention than before both experimentally and theoretically.[1] The study of the exclusive charmless B decays is very interesting for several reasons. First of all, they proceed in general through the W-loop diagram (the so-called penguin diagram is its one-gluon approximation) without suffering from the Kobayashi-Maskawa (KM) mixing suppression, and through the spectator diagrams with KM mixing double suppression. This becomes a salient feature in charmless B decay: loop graphs are as important as or even dominate over tree graphs. Moreover, there exist some decay modes which occur solely via the W-loop diagram, e.g., $B_d^0 \to \phi K^0, B_s^0 \to \phi \bar{K}^0$. The W-loop diagrams play an essential role in kaon system: In the KM model it is responsible for the direct CP violation characterized by the parameter ϵ'; its contribution at low energies (i.e., the so-called "eye" graph) could partially account for the mysterious $\Delta I = \frac{1}{2}$ rule.[2,3] In spite of its importance, the penguin contribution in K decay is still under intense study and debate. Therefore, the measurement of two-body charmless B decays can provide a unique and excellent test on the penguin mechanism and shed some light on QCD calculations.

Charmless exclusive two-body decays of B mesons and their CP asymmetries have been systematically studied in Ref. 1 (see also Refs. 4–6). Nevertheless, we wish to update and reanalyze in this paper the rare B decays in more detail, motivated by the following observations. (i) A new lower bound on the top-quark mass, $m_t > 77$ GeV, was set by the Collider Detector at Fermilab (CDF) Collaboration.[7] This means that the full effects of the top quark and W boson in W-loop diagrams should be taken into consideration. (ii) The ratio of the KM mixing angles $|V_{ub}/V_{cb}|$ was recently extracted, though model dependently, from the charmless semileptonic B decays by both ARGUS[8] and CLEO[9] Collaborations. (iii) Form factors such as $f_+(0)$ in the matrix element of $\langle P_1|V_\mu|P_2\rangle$ were taken to be unity in Ref. 1. As a result, the predicted branching ratio of, e.g., $B_d^0 \to \pi^+\pi^-$ already exceeds the present upper limit. This indicates that it is important to adopt some phenomenological models for form factors as an input for theoretical calculations.

In the light of the above-mentioned developments, we reinvestigated the exclusive charmless decays of B mesons. This paper is organized as follows. We first set up in Sec. II the framework necessary for subsequent studies. In Sec. III we discuss the use of quark-diagram amplitude scheme. The quark-diagram representations and the numerical results of two-body charmless B decays are given in Tables II–VII. Three examples of detailed evaluation of the decay rates are presented in Sec. IV. Summary and conclusions are given in Sec. V.

II. FRAMEWORK

A. Effective Hamiltonian

The standard effective weak Hamiltonian for W tree graphs relevant for charmless B decays reads

$$H_{\rm eff} = \frac{G_F}{\sqrt{2}} V_{us} V_{ub}^* (c_+ O_+ + c_- O_-) + (s \to d) + \text{H.c.} , \tag{2.1}$$

with

$$O_\pm = \tfrac{1}{2}[(\bar{s}u)(\bar{u}b) \pm (\bar{u}u)(\bar{s}b)] , \tag{2.2}$$

where $(\bar{q}_1 q_2) = \bar{q}_1 \gamma_\mu (1-\gamma_5) q_2$, $c_\pm$ are QCD-corrected Wilson coefficient functions, and V_{ij}'s are the KM-mixing-matrix elements. The effective Hamiltonian for the W-loop penguin interaction in the 't Hooft–Feynman gauge is

$$H_{\rm peng}=\sqrt{2}G_F\left[\frac{\alpha_s}{2\pi}\right]\left[\sum V_{ib}^*V_{is}I_i\right](\bar{s}_L\gamma_\mu\lambda^a b_L)(\bar{q}\gamma_\mu\lambda^a q)+(s\to d)+\text{H.c.}\ , \tag{2.3}$$

where the dipole-moment contributions are negligible, and the loop integral I_i is given by

$$I_i=\frac{1}{1-x_i}\left[1+\frac{x_i}{2}\right]\left[\int_0^1 dz\, z(1-z)\ln[m_i^2-k^2z(1-z)]-\int_0^1 dz\, z(1-z)\ln[M_W^2(1-z)+m_i^2z-k^2z(1-z)]\right], \tag{2.4}$$

where $x_i=m_i^2/M_W^2$, m_i is the mass of the ith-type loop quark, and k^2 is the momentum transfer carried by the gluon that was first derived in Ref. 4 and Eq. (2.4) has the exact quark-mass terms, which we have double checked and agreed. Notice that the loop integral I_i is smooth at $x_i=1$.

The momentum-squared k^2 of the gluon can be either timelike or spacelike, depending on the way the final state is being formed. Since k^2 in the B system is of order m_b^2, a timelike penguin diagram involving u and c quarks will have an absorptive part, which is crucial for generating CP asymmetries in B decay, as first noticed in Ref. 10. It is easily seen from Eq. (2.4) that, when $k^2>4m_i^2$,

$$\text{Im}I_i=-\frac{1}{6}\pi\left[1+\frac{2m_i^2}{k^2}\right]\left[1-\frac{4m_i^2}{k^2}\right]^{1/2}. \tag{2.5}$$

The penguin-induced effective Hamiltonian is usually recast into the form

$$H_{\rm peng}=\frac{G_F}{\sqrt{2}}\frac{\alpha_s}{\pi}\left[\sum\lambda_i I_i\right][-\tfrac{2}{3}(\bar{s}_L^\alpha\gamma_\mu q_L^\beta)(\bar{q}_L^\beta\gamma^\mu b_L^\alpha)+2(\bar{s}_L^\alpha\gamma_\mu q_L^\alpha)(\bar{q}_L^\beta\gamma^\mu b_L^\beta)$$
$$+\tfrac{4}{3}(\bar{s}_L^\alpha q_R^\beta)(\bar{q}_R^\beta b_L^\alpha)-4(\bar{s}_L^\alpha q_R^\alpha)(\bar{q}_R^\beta b_L^\beta)]+(s\to d)+\text{H.c.}\ , \tag{2.6}$$

where a Fierz transformation has been made for the $(V-A)(V+A)$ part of the interaction, $\lambda_i=V_{ib}^*V_{is}$, and α,β are color indices. Note that the renormalization-group effect has not been included in Eq. (2.6). In the case that $M_W^2\gg m_t^2\gg k^2\sim m_b^2$, one can neglect the second logarithmic term in I_i and obtain

$$\left[\frac{\alpha_s}{2\pi}\right]\left[\sum\lambda_i I_i\right]\approx\frac{\alpha_s}{12\pi}\left[\lambda_t\left[\ln\frac{m_t^2}{k^2}+\frac{5}{3}+i\pi\right]-\lambda_c\frac{m_c^2}{k^2}-\lambda_u\frac{m_u^2}{k^2}\right] \tag{2.7}$$

to a good approximation. Indeed, the penguin contribution was crudely estimated to be of order $(\alpha_s/12\pi)\ln(m_t^2/m_b^2)$ in the early literature.[11] Nowadays, the larger value of m_t demands the necessity of using the exact expression of I_t in order to fully comprehend the effect of the top quark and W boson. The dispersive and absorptive parts of I_i are depicted in Table I for given values of k^2 and m_t.

It is instructive to consider the penguin operator in the kaon system. Since there k^2 is of order m_K^2, one may neglect it in the second logarithmic term of Eq. (2.4) (with the b quark being replaced by the d quark). It is not difficult to show that the penguin coefficient function reads[12,13]

$$c_5(\mu)=-\left[\frac{\alpha_s}{12\pi}\right]\left[\ln\frac{m_c^2}{\mu^2}+\frac{5}{3}\right]+\frac{V_{td}V_{ts}^*}{V_{ud}V_{us}^*}\left[\frac{\alpha_s}{12\pi}\right]\left[\ln\frac{m_t^2}{m_c^2}-D(x_t)\right]\left[1+\frac{x_t}{2}\right], \tag{2.8}$$

where

$$D(x)=\frac{x}{8(1-x)^3}(18-11x-x^2)+\frac{x^2\ln x}{4(1-x)^4}(15-16x+4x^2)\ . \tag{2.9}$$

The first term of $c_5(\mu)$ is the well-known real part of the penguin coefficient,[13] whereas direct CP violation in $K\to\pi\pi$ decay characterized by the parameter ϵ' is governed by the second term. [As far as we know, the factor of $(1+m_t^2/2M_W^2)$ in the imaginary part of the penguin coefficient, which becomes important as m_t increases, was so far not considered in the literature.] Unfortunately, we only know how to compute the penguin coefficient perturbatively down to the scale $\mu\sim 1$ GeV. At the energy scale relevant for kaon decay, the evaluation of Wilson coefficients is a nonperturbative question beyond our present ability. This feature makes the study of kaon nonleptonic decay profoundly difficult. By contrast, the penguin loop in charmless B decay is dominated by the t quark, and hence it provides a more interesting case to test the short-distance QCD calculations.

B. Form factors

We shall use the factorization method to evaluate the rare B decay amplitude. In the naive vacuum-insertion approximation, a factor of $(2c_+ +c_-)/3$ is gained by the color-matched decay mode, while the QCD-corrected factor $(2c_+ -c_-)/3$ is always associated with the color-mismatched channels (e.g., $D^0\to\bar{K}^0\pi^0$). It is well known that the predictions based on the conventional vacuum-saturation method are grossly inconsistent with data for

color-suppressed modes.[14] This discrepancy is improved in the so-called $1/N_c$ expansion[15] (N_c being the number of colors), in which the Fierz-transformed contributions characterized by the color factor $1/N_c$ are dropped in the large-N_c approximation. This amounts to replacing $(2c_+ - c_-)/3$ by $(c_+ - c_-)/2$ and $(2c_+ + c_-)/3$ by $(c_+ + c_-)/2$.

The $1/N_c$ approach is known to be working well for charm decay but it has not been critically tested in B decay as data are still not as accurate as that of charm decay. Nevertheless, we find in the factorization method that the ARGUS and CLEO data for the color-suppressed channels $B_u^+ \to \psi K^+, \psi K^{*+}$, $B_d^0 \to \psi K^0, \psi K^{*0}$ and the inclusive decay $B \to \psi + X$ are satisfactorily explained provided that (see Appendix A)

$$\tfrac{1}{3}(2c_+ - c_-) \approx -0.25 , \tag{2.10a}$$

which is to be compared with the naive value of $(2c_+ - c_-)/3 \approx 0.05$ and the $1/N_c$ prediction $(c_+ - c_-)/2 \approx -0.34$ for the representative values $c_+ = 0.82$ and $c_- = 1.49$. It is evident that the $1/N_c$ expectation is closer to reality. So we take the standard strategy of the factorization formalism and the phenomenological value for $(2c_+ - c_-)/3$ as given by Eq. (2.10a), but keep the theoretical value for

$$(2c_+ + c_-)/3 = 1.04 . \tag{2.10b}$$

Under the assumption of factorization, the decay amplitude is decomposed into the product of one- and two-body hadronic matrix elements. We first fix the convention for the one-body matrix element of the axial-vector current to be

$$\langle P(q)|A_\mu|0\rangle = -if_P q_\mu, \quad \langle 0|A_\mu|P(q)\rangle = if_P q_\mu . \tag{2.11}$$

TABLE I. The dispersive absorptive parts of the loop integral function I_i given by Eq. (2.4) as a function of k^2 and m_t. The function I_t is rather insensitive to the value of k^2.

	Timelike ($k^2>0$)		Spacelike ($k^2<0$)	
$\lvert k^2/m_b^2\rvert$	I_u	I_c	I_u	I_c
1.00	$-1.066-i0.523$	$-1.222-i0.494$	-1.067	-1.000
0.95	$-1.075-i0.523$	$-1.197-i0.489$	-1.076	-1.006
0.90	$-1.084-i0.523$	$-1.213-i0.489$	-1.084	-1.012
0.85	$-1.093-i0.523$	$-1.243-i0.475$	-1.094	-1.018
0.80	$-1.104-i0.523$	$-1.252-i0.475$	-1.104	-1.024
0.75	$-1.114-i0.523$	$-1.286-i0.475$	-1.115	-1.031
0.70	$-1.126-i0.523$	$-1.300-i0.460$	-1.126	-1.038
0.65	$-1.138-i0.523$	$-1.329-i0.443$	-1.139	-1.045
0.60	$-1.152-i0.523$	$-1.364-i0.425$	-1.152	-1.052
0.55	$-1.166-i0.523$	$-1.399-i0.405$	-1.166	-1.060
0.50	$-1.182-i0.523$	$-1.446-i0.383$	-1.182	-1.069
0.45	$-1.200-i0.523$	$-1.501-i0.336$	-1.200	-1.077
0.40	$-1.219-i0.523$	$-1.574-i0.229$	-1.219	-1.087
0.35	$-1.241-i0.523$	$-1.521-i0.000$	-1.242	-1.097
0.30	$-1.267-i0.523$	$-1.395-i0.000$	-1.267	-1.107
0.25	$-1.298-i0.523$	$-1.334-i0.000$	-1.298	-1.118
0.20	$-1.335-i0.523$	$-1.292-i0.000$	-1.335	-1.131
0.15	$-1.383-i0.523$	$-1.260-i0.000$	-1.383	-1.144
0.10	$-1.450-i0.523$	$-1.233-i0.000$	-1.450	-1.158

m_t (GeV)	I_t
70	-0.140
80	-0.126
90	-0.116
100	-0.108
110	-0.102
120	-0.097
130	-0.093
140	-0.090
150	-0.087
160	-0.085
170	-0.083
180	-0.082
190	-0.081
200	-0.079

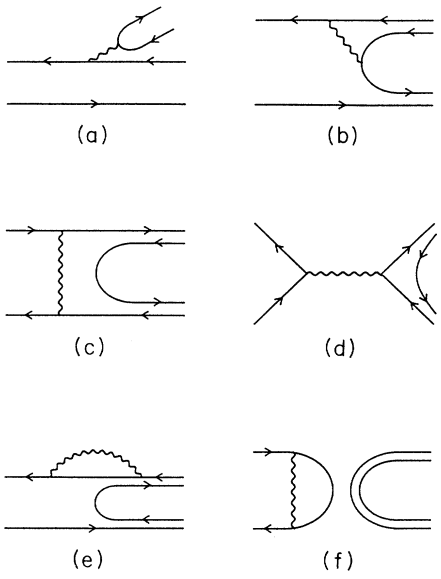

FIG. 1. The six quark diagrams for a meson decaying into two mesons.

The decay constants relevant for our purposes are

$$f_\pi = 132 \text{ MeV}, \quad f_K = 160 \text{ MeV}, \quad f_{B_u} \approx 120 \text{ MeV} . \tag{2.12}$$

The estimate of the decay constant for B_u^+ is still subject to controversy. A recent lattice evaluation yields[16] $f_{B_u} = 105 \pm 20 \pm 35$ MeV. In this paper we will use the representative value 120 MeV. As we shall see in Sec. IV, the choice of f_{B_u} is immaterial since it is relevant only for the annihilation amplitude which is suppressed with respect to the spectator amplitude. Taking into account SU(3) breaking and η_0-η_8 mixing, the η and η' decay constants are (see Appendix B)

$$\begin{aligned} &\langle 0|(\bar{u}u)|\eta\rangle = \langle 0|(\bar{d}d)|\eta\rangle \simeq iq_\mu (92 \text{ MeV}) , \\ &\langle 0|(\bar{s}s)|\eta\rangle \simeq iq_\mu (-105 \text{ MeV}) , \\ &\langle 0|(\bar{u}u)|\eta'\rangle = \langle 0|(\bar{d}d)|\eta'\rangle \simeq iq_\mu (49 \text{ MeV}) , \\ &\langle 0|(\bar{s}s)|\eta'\rangle \simeq iq_\mu (120 \text{ MeV}) . \end{aligned} \tag{2.13}$$

The one-body hadronic matrix element of the vector current is parametrized as

$$\langle 0|V_\mu|V(q)\rangle = f_V m_V^2 \epsilon_\mu . \tag{2.14}$$

The dimensionless vector coupling f_V of the neutral vector meson V is determined by the observed leptonic decay rate of $V \to e^+e^-$. We find

$$f_{\rho^0} = 0.203, \quad f_\omega = 0.185, \quad f_\phi = -0.228 . \tag{2.15}$$

For K^* and the charged ρ meson, we set

$$f_{\rho^+} = f_{K^*} = \sqrt{2} f_{\rho^0} = 0.287 . \tag{2.16}$$

The general expression for the pseudoscalar-pseudoscalar matrix element reads

$$\langle P_2(p_2)|V_\mu|P_1(p_1)\rangle = f_+(t)(p_1+p_2)_\mu + f_-(t)(p_1-p_2)_\mu , \tag{2.17}$$

where $t = (p_1-p_2)^2$. The sign of f_+ can be fixed using the soft-pion (or soft-meson) theorem and Eq. (2.11). For example, it is easily shown that the form factor f_+ of $\langle \pi^-|(\bar{s}u)|K^0\rangle$ is negative, while it is positive in the matrix element of $\langle \pi^+|(\bar{u}s)|\bar{K}^0\rangle$. There are basically two different approaches for the form factors.[17] The first type of model[18] assumes nearest pole dominance for the q^2 dependence of the form factors

$$|f_\pm(q^2)| \simeq \frac{h_\pm}{1 - q^2/m_{\text{pole}}^2} , \tag{2.18}$$

where the unknown form factors $h_\pm$ at $q^2=0$ are estimated by describing the mesons as relativistic bound states of a quark-antiquark pair in the infinite-momentum frame. Nonrelativistic quark potential method is utilized in the second approach[19] to make a correspondence between the form factors defined in Eqs. (2.18) and (2.21) and those appearing in a quark-model calculation. Form factors are identified near zero recoil and an extrapolation away from zero recoil is required.

In this paper we will use the form factors of Bauer, Stech, and Wirbel[5] (BSW) for h_+. As for the other form factor $f_-(t)$, we adopt the ansatz derived from the constituent U(2,2) quark model[20]

$$f_-(t) = -\frac{m_1 - m_2}{m_1 + m_2} f_+(t) . \tag{2.19}$$

Although the form factor f_- in heavy-meson decay is numerically as important as f_+, its contribution to the decay amplitude is usually suppressed by the heavy-quark mass squared. Moreover, it does not contribute to $B \to VP$ decay in the factorizable approximation.

In evaluating the W-exchange or W-annihilation diagram, one will encounter matrix elements, e.g., $\langle \pi^+ K^0|(\bar{u}s)|0\rangle$ to be evaluated at $q^2 = m_B^2$. So far there is no reliable way to estimate those form factors; the dipole q^2 behavior given by Eq. (2.18) is no longer valid at such a large momentum transfer. The approach taken by Refs. 5 and 15 was to ignore them based on helicity-suppression arguments (as in $\pi \to e\bar{\nu}_e$). However, such naive assumptions had met gross inconsistency comparing with data on $D \to PV$.[14] Here we have no good suggestions except to drop these W exchange and W annihilation graphs in our numerical calculations and discuss in what reactions we can test the importance of these nonspectator diagrams.

The pseudoscalar-vector matrix element is parametrized as

$$\begin{aligned} &\langle V(p_2)|V_\mu + A_\mu|P(p_1)\rangle \\ &\quad = \epsilon_{\mu\nu\rho\sigma}\epsilon_2^\nu p_1^\rho p_2^\sigma F^V(t) \\ &\qquad + i\epsilon_2^\nu [g_{\mu\nu} F_1^A(t) + p_{1\mu} p_{1\nu} F_2^A(t) + p_{2\mu} p_{1\nu} F_3^A(t)] . \end{aligned} \tag{2.20}$$

We use the form factors of BSW,[5] namely,

$$F_1^A(t)=(m_V+m_P)A_1(t)\ ,$$
$$F_2^A(t)=F_3^A(t)=-\frac{1}{m_V+m_P}A_2(t)\ , \qquad (2.21)$$
$$F^V(t)=\frac{2}{m_V+m_P}V(t)\ ,$$

which are also the predictions of the U(2,2) quark model.[21] In the notation of BSW, $A_1(0)=h_{A_1}$, $A_2(0)=h_{A_2}$, and $V(0)=h_V$. The most sensitive test on the VP form factors is provided by the recent Mark III data[22] on $D\to\bar{K}^{*}\rho$: not only the absolute rates but also the angular correlations are being measured. We find that the branching ratio of $D^+\to\bar{K}^{*0}\rho^+$ and the relative contribution of the longitudinal and transverse transitions to the decay rate are well explained within the framework of the $1/N_c$ factorization approach in conjunction with the VP form factors given by Eq. (2.21). The detailed analysis will be presented elsewhere.

Before proceeding we wish to stress that although the form factors of BSW are employed in Eqs. (2.18) and (2.21), the present analysis is different from that of BSW in one crucial respect: penguin graphs, which play an essential role in rare B decays, were not taken into consideration by BSW.

B. KM matrix elements

A convenient parametrization of the quark mixing matrix is that of Chau and Keung, which has been adopted by the Particle Data Group,[23a]

$$V=\begin{array}{c}\begin{matrix} d & s & b \end{matrix}\\ \begin{pmatrix} c_xc_z & s_xc_z & s_ze^{-i\phi} \\ -s_xc_y-c_xs_ys_ze^{i\phi} & c_xc_y-s_xs_ys_ze^{i\phi} & s_yc_z \\ s_xs_y-c_xc_ys_ze^{i\phi} & -c_xs_y-s_xc_ys_ze^{i\phi} & c_yc_z \end{pmatrix}\end{array}\begin{matrix} u \\ c \\ t \end{matrix}\ , \qquad (2.22)$$

where $c_x=\cos\theta_x, s_x=\sin\theta_x, \ldots$. A nice feature of this parametrization is that each angle is directly related to a class of experimental measurements: $|V_{us}|\approx s_x\approx 0.22$, from strange particle decay; $|V_{cb}|\approx s_y\approx 0.05$, from b-lifetime measurements; $|V_{ub}|\approx s_z\approx 0.005$, from experiment on $(b\to u)/(b\to c)$. Setting $s_x=\lambda=0.22$, $s_y=A\lambda^2$, and $s_z\exp(-i\phi)=A\lambda^3(\rho-i\eta)$, we find that, to a good approximation, Eq. (2.22) is reduced to

$$V=\begin{pmatrix} 1-\frac{1}{2}\lambda^2 & \lambda & A\lambda^3(\rho-i\eta) \\ -\lambda+\cdots & 1-\frac{1}{2}\lambda^2+\cdots & A\lambda^2 \\ A\lambda^3(1-\rho-i\eta) & -A\lambda^2+\cdots & 1 \end{pmatrix}\ , \qquad (2.23)$$

which is precisely the well-known Wolfenstein parametrization.[24] The parameter A is fixed by the measured V_{cb} to be[25] 1.0 ± 0.1. The parameters ρ and η are subject to the constraint[25] $(\rho^2+\eta^2)^{1/2}=0.46\pm 0.23$ for $|V_{ub}/V_{cb}|=0.10\pm 0.05$. If m_t is of order 100 GeV, ρ is constrained to be negative[25,26] by the observed B_d^0-$\bar{B}_d^0$ mixing at ARGUS and CLEO, but a positive ρ is equally allowed if the top quark is very heavy, $m_t\gtrsim 200$ GeV. For our purposes, we take

$$\rho=-0.40,\quad \eta=0.25\ , \qquad (2.24)$$

which correspond to $|V_{ub}/V_{cb}|=0.1$, and are consistent with current experiments on $B^0-\bar{B}^0$ mixing and ϵ'/ϵ.

Note that in order to obtain the correct CP noninvariance those dropped ellipsis terms in Eq. (2.23) must be included. Otherwise serious mistakes can be made, e.g., charm quark would not contribute to CP noninvariance in K decays, and Gilman and Wise would not have discovered the Σ' effect from the KM matrix. It is therefore better to use the precise parametrization of Eq. (2.22).

III. QUARK-DIAGRAM AMPLITUDES

Before embarking on the theoretical calculation, we shall express all charmless $B^{\pm}$ decays in terms of six distinct quark diagrams (see Fig. 1) (Refs. 27 and 14): $\mathcal{A}$, the external W-emission diagram; $\mathcal{B}$, the internal W-emission diagram; $\mathcal{C}$, the W-exchange diagram; $\mathcal{D}$, the W-annihilation diagram; $\mathcal{E}$, the horizontal W-loop diagram; $\mathcal{F}$, the vertical W-loop diagram. (The one-gluon-exchange approximation of the $\mathcal{E}$ graph is the so-called "penguin diagram.") These quark diagrams are classified according to the topology of weak interactions with all QCD strong-interaction effects included. The quark-diagram amplitudes for all charmless exclusive two-body modes of B mesons without SU(3) breaking and final-state interactions are listed in Tables II–VII. For final states involving η or η', we apply the wave function given by Eq. (B6).

The use of the quark-diagram scheme enables us to gain some salient features of rare B decays before performing realistic calculations. A quick scan over Tables II–VII clearly shows that the horizontal W-loop diagram contributes to all exclusive charmless B decays except for $B_u^+\to\pi^+\pi^0,\rho^+\rho^0,a_1^+a_1^0$ in which W-loop contributions are canceled out. It is interesting to note that only the vertical W-loop diagram contributes to $B_d^0\to\phi\eta,\phi\eta',\phi\phi$.

On a close scrutiny, we see that rare charged B decays can be classified into three different categories.

(i) Decay modes primarily dominated by the horizontal W-loop diagrams. There exist many such examples: $B_u^+\to K^0\pi^+,K^+\bar{K}^0,K^+\phi,\ldots$; $B_d^0\to K^0\pi^0,K^0\omega,\ldots$. Moreover, as pointed out in the Introduction and Ref. 14, there are some neutral B decay modes which occur solely via the W-loop diagrams, e.g., $B_d^0\to\phi K^0$, $B_s^0\to\phi\bar{K}^0$, $B_{d,s}^0\to\phi\phi,K^0\bar{K}^0,\ldots$.

TABLE II. Quark-diagram amplitudes, branching ratios for charmless exclusive $B \to PP$ decays. The underlined W-loop amplitudes refers to the graph with $\bar{s}s$ in between. Some decay modes have two different timelike penguin diagrams due to the existence of two inbetween quark-antiquark states, namely, $\bar{u}u$ and $\bar{d}d$; experimental limits are taken from Refs. 28–30. Owing to the large uncertain factor of $m_B^2/[(m_b+m_u)(m_d-m_u)]$, the branching ratios (BR's) of $B_u^+ \to \pi^+\eta$ and $\pi^+\eta'$ are listed in the table without including the contributions from spacelike penguin diagrams.

Reaction	Amplitude				$(\mathrm{Br})_{\mathrm{theory}}$	Expt. limits from ARGUS	Expt. limits from CLEO
$B_d^0 \to K^+\pi^-$	$V_{us}V_{ub}^*$	$(\mathcal{A}+\mathcal{E}_{u-c})$	$+V_{ts}V_{tb}^*$	$(\mathcal{E}_{t-c})$	1.7×10^{-5}	1.8×10^{-4}	0.9×10^{-4}
$\to K^0\bar{K}^0$	$V_{ud}V_{ub}^*$	$(\mathcal{E}_{u-c}+\mathcal{J}_{u-c})$	$+V_{td}V_{tb}^*$	$(\mathcal{E}_{t-c}+\mathcal{J}_{t-c})$	1.2×10^{-6}		
$\to K^0\pi^0$	$V_{us}V_{ub}^*\frac{1}{\sqrt{2}}$	$(\mathcal{B}-\mathcal{E}_{u-c})$	$+V_{ts}V_{tb}^*\frac{1}{\sqrt{2}}$	$(-\mathcal{E}_{t-c})$	6.0×10^{-6}		
$\to K^0\eta$	$V_{us}V_{ub}^*\frac{1}{\sqrt{3}}$	$(\mathcal{B}+\underline{\mathcal{E}}_{u-c}-\mathcal{E}_{u-c})$	$+V_{ts}V_{tb}^*\frac{1}{\sqrt{3}}$	$(\underline{\mathcal{E}}_{t-c}-\mathcal{E}_{t-c})$	1.7×10^{-6}		
$\to K^0\eta'$	$V_{us}V_{ub}^*\frac{1}{\sqrt{6}}$	$(\mathcal{B}+\underline{\mathcal{E}}_{u-c}+2\mathcal{E}_{u-c})$	$+V_{ts}V_{tb}^*\frac{1}{\sqrt{6}}$	$(\underline{\mathcal{E}}_{t-c}+2\mathcal{E}_{t-c})$	2.9×10^{-5}		
$\to \pi^+\pi^-$	$V_{ud}V_{ub}^*$	$(\mathcal{A}+\mathcal{C}+\mathcal{E}_{u-c}+\mathcal{J}_{u-c})$	$+V_{td}V_{tb}^*$	$(\mathcal{E}_{t-c}+\mathcal{J}_{t-c})$	1.3×10^{-5}	1.3×10^{-4}	0.9×10^{-4}
$\to \pi^0\pi^0$	$V_{ud}V_{ub}^*\frac{1}{2}$	$(-\mathcal{B}+\mathcal{C}+\mathcal{E}_{u-c}+\mathcal{J}_{u-c})$	$+V_{td}V_{tb}^*\frac{1}{2}$	$(\mathcal{E}_{t-c}+\mathcal{J}_{t-c})$	1.0×10^{-6}		
$\to \pi^0\eta$	$V_{ud}V_{ub}^*\frac{1}{\sqrt{6}}$	$(\underline{\mathcal{B}}-\mathcal{B}+\underline{\mathcal{C}}-\mathcal{C}-\underline{\mathcal{E}}_{u-c}-\mathcal{E}_{u-c})$	$+V_{td}V_{tb}^*\frac{1}{\sqrt{6}}$	$(-\underline{\mathcal{E}}_{t-c}-\mathcal{E}_{t-c})$	4.1×10^{-6}	1.8×10^{-3}	
$\to \pi^0\eta'$	$V_{ud}V_{ub}^*\frac{1}{2\sqrt{3}}$	$(\underline{\mathcal{B}}-\mathcal{B}+\underline{\mathcal{C}}+\mathcal{C}-\underline{\mathcal{E}}_{u-c}-\mathcal{E}_{u-c})$	$+V_{td}V_{tb}^*\frac{1}{2\sqrt{3}}$	$(-\underline{\mathcal{E}}_{t-c}-\mathcal{E}_{t-c})$	1.3×10^{-5}		
$\to \eta\eta$	$V_{ud}V_{ub}^*\frac{1}{3}$	$(\mathcal{B}+\mathcal{C}+\mathcal{E}_{u-c}+\mathcal{J}_{u-c})$	$+V_{td}V_{tb}^*\frac{1}{3}$	$(\mathcal{E}_{t-c}+\mathcal{J}_{t-c})$	1.4×10^{-5}		
$\to \eta\eta'$	$V_{ud}V_{ub}^*\frac{1}{3\sqrt{2}}$	$(\mathcal{B}+\underline{\mathcal{B}}+\mathcal{C}+\underline{\mathcal{C}}+\mathcal{E}_{u-c}+\underline{\mathcal{E}}_{u-c})$	$+V_{td}V_{tb}^*\frac{1}{3\sqrt{2}}$	$(\mathcal{E}_{t-c}+\mathcal{E}_{t-c})$	4.2×10^{-5}		
$\to \eta'\eta'$	$V_{ud}V_{ub}^*\frac{1}{6}$	$(\mathcal{B}+\mathcal{C}+\mathcal{E}_{u-c}+6\mathcal{J}_{u-c})$	$+V_{td}V_{tb}^*\frac{1}{6}$	$(\mathcal{E}_{t-c}+6\mathcal{J}_{t-c})$	3.0×10^{-5}		
$B_u^+ \to K^+\pi^0$	$V_{us}V_{ub}^*\frac{1}{\sqrt{2}}$	$(\mathcal{A}+\mathcal{B}+\mathcal{D}+\mathcal{E}_{u-c})$	$+V_{ts}V_{tb}^*\frac{1}{\sqrt{2}}$	$(\mathcal{E}_{t-c})$	8.1×10^{-6}		
$\to K^0\pi^+$	$V_{us}V_{ub}^*$	$(\mathcal{D}+\mathcal{E}_{u-c})$	$+V_{ts}V_{tb}^*$	$(\mathcal{E}_{t-c})$	1.2×10^{-5}	1.0×10^{-4}	9.0×10^{-5}
$\to K^+\bar{K}^0$	$V_{ud}V_{ub}^*$	$(\mathcal{D}+\mathcal{E}_{u-c})$	$+V_{td}V_{tb}^*$	$(\mathcal{E}_{t-c})$	1.0×10^{-6}		
$\to K^+\eta$	$V_{us}V_{ub}^*\frac{1}{\sqrt{3}}$	$(\mathcal{A}+\mathcal{B}+\mathcal{D}-\underline{\mathcal{D}}+\mathcal{E}_{u-c}-\underline{\mathcal{E}}_{u-c})$	$+V_{ts}V_{tb}^*\frac{1}{\sqrt{3}}$	$(\mathcal{E}_{t-c}-\underline{\mathcal{E}}_{t-c})$	4.5×10^{-6}		
$\to K^+\eta'$	$V_{us}V_{ub}^*\frac{1}{\sqrt{6}}$	$(\mathcal{A}+\mathcal{B}+\mathcal{D}-2\underline{\mathcal{D}}+\mathcal{E}_{u-c}+2\underline{\mathcal{E}}_{u-c})$	$+V_{ts}V_{tb}^*\frac{1}{\sqrt{6}}$	$(\mathcal{E}_{t-c}+2\underline{\mathcal{E}}_{t-c})$	3.6×10^{-5}		
$\to \pi^+\pi^0$	$V_{ud}V_{ub}^*\frac{1}{\sqrt{2}}$	$(\mathcal{A}+\mathcal{B})$			6.0×10^{-6}	2.4×10^{-4}	
$\to \pi^+\eta$	$V_{ud}V_{ub}^*\frac{1}{\sqrt{3}}$	$(\mathcal{A}+\mathcal{B}+2\mathcal{D}+\mathcal{E}_{u-c}+\underline{\mathcal{E}}_{u-c})$	$+V_{td}V_{tb}^*\frac{1}{\sqrt{3}}$	$(\mathcal{E}_{t-c}+\underline{\mathcal{E}}_{t-c})$	5.6×10^{-6}	7.0×10^{-4}	
$\to \pi^+\eta'$	$V_{ud}V_{ub}^*\frac{1}{\sqrt{6}}$	$(\mathcal{A}+\mathcal{B}+2\mathcal{D}+\mathcal{E}_{u-c}+\underline{\mathcal{E}}_{u-c})$	$+V_{td}V_{tb}^*\frac{1}{\sqrt{6}}$	$(\mathcal{E}_{t-c}+\underline{\mathcal{E}}_{t-c})$	1.5×10^{-5}		

TABLE III. Same as Table II except for $B \to VP$ decays. The primed amplitudes denote the case when the vector meson comes directly from the b decay. (Note that we use the same generic notation $\mathcal{A}, \mathcal{B}, \mathcal{C}, \mathcal{D}, \mathcal{E}, \mathcal{F}$, but they are not related to those for $B \to PP$. Similar comments apply to Tables IV–VII.)

Reaction	Amplitude				$(\mathrm{Br})_{\mathrm{theory}}$	Expt. limits from ARGUS	Expt. limits from CLEO
$B_d^0 \to K^{*0} K^0$	$V_{ud} V_{ub}^*$	$(\mathcal{E}_{u-c} + \mathcal{F}_{u-c})$	$+ V_{td} V_{tb}^*$	$(\mathcal{E}_{t-c} + \mathcal{F}_{t-c})$	3.9×10^{-8}		
$\to K^0 \bar{K}^{*0}$	$V_{ud} V_{ub}^*$	$(\mathcal{E}'_{u-c} + \mathcal{F}_{u-c})$	$+ V_{td} V_{tb}^*$	$(\mathcal{E}'_{t-c} + \mathcal{F}_{t-c})$	1.0×10^{-6}		
$\to K^+ \rho^-$	$V_{us} V_{ub}^*$	$(\mathcal{A}' + \mathcal{E}_{u-c})$	$+ V_{ts} V_{tb}^*$	$(\mathcal{E}_{t-c})$	1.9×10^{-6}		
$\to K^0 \rho^0$	$V_{us} V_{ub}^* \frac{1}{\sqrt{2}}$	$(\mathcal{B}' - \mathcal{E}_{u-c})$	$+ V_{ts} V_{tb}^* \frac{1}{\sqrt{2}}$	$(-\mathcal{E}_{t-c})$	3.5×10^{-7}	1.6×10^{-4}	5.8×10^{-4}
$\to K^{*+} \pi^-$	$V_{us} V_{ub}^*$	$(\mathcal{A} + \mathcal{E}'_{u-c})$	$+ V_{ts} V_{tb}^*$	$(\mathcal{E}'_{t-c})$	1.9×10^{-5}	6.2×10^{-4}	4.4×10^{-4}
$\to K^{*0} \pi^0$	$V_{us} V_{ub}^* \frac{1}{\sqrt{2}}$	$(\mathcal{B} - \mathcal{E}'_{u-c})$	$+ V_{ts} V_{tb}^* \frac{1}{\sqrt{2}}$	$(-\mathcal{E}'_{t-c})$	4.7×10^{-6}		
$\to K^0 \phi$	$V_{us} V_{ub}^*$	$(\mathcal{E}'_{u-c})$	$+ V_{ts} V_{tb}^*$	$(\mathcal{E}'_{t-c})$	8.9×10^{-6}	3.6×10^{-4}	4.9×10^{-4}
$\to K^0 \omega$	$V_{us} V_{ub}^* \frac{1}{\sqrt{2}}$	$(\mathcal{B}' + \mathcal{E}_{u-c})$	$+ V_{ts} V_{tb}^* \frac{1}{\sqrt{2}}$	$(\mathcal{E}_{t-c})$	1.1×10^{-7}		
$\to K^{*0} \eta$	$V_{us} V_{ub}^* \frac{1}{\sqrt{3}}$	$(\mathcal{B} - \mathcal{E}_{u-c} + \mathcal{E}'_{u-c})$	$+ V_{ts} V_{tb}^* \frac{1}{\sqrt{3}}$	$(-\mathcal{E}_{t-c} + \mathcal{E}'_{t-c})$	4.5×10^{-6}		
$\to K^{*0} \eta'$	$V_{us} V_{ub}^* \frac{1}{\sqrt{6}}$	$(\mathcal{B} + 2\mathcal{E}_{u-c} + \mathcal{E}'_{u-c})$	$+ V_{ts} V_{tb}^* \frac{1}{\sqrt{6}}$	$(2\mathcal{E}_{t-c} + \mathcal{E}'_{t-c})$	3.4×10^{-6}		
$\to \rho^+ \pi^-$	$V_{ud} V_{ub}^*$	$(\mathcal{A} + \mathcal{C} + \mathcal{E}'_{u-c} + \mathcal{F}_{u-c})$	$+ V_{td} V_{tb}^*$	$(\mathcal{E}'_{t-c} + \mathcal{F}_{t-c})$	3.9×10^{-5}	5.2×10^{-4}	
$\to \rho^- \pi^+$	$V_{ud} V_{ub}^*$	$(\mathcal{A}' + \mathcal{C}' + \mathcal{E}_{u-c} + \mathcal{F}_{u-c})$	$+ V_{td} V_{tb}^*$	$(\mathcal{E}_{t-c} + \mathcal{F}_{t-c})$	1.1×10^{-5}		
$\to \rho^0 \pi^0$	$V_{ud} V_{ub}^* \frac{1}{2}$	$(-\mathcal{B} - \mathcal{B}' + \mathcal{C} + \mathcal{C}' + \mathcal{E}_{u-c} + \mathcal{E}'_{u-c})$	$+ V_{td} V_{tb}^* \frac{1}{2}$	$(\mathcal{E}_{t-c} + \mathcal{E}'_{t-c})$	2.3×10^{-6}	4.0×10^{-4}	
$\to \rho^0 \eta$	$V_{ud} V_{ub}^* \frac{1}{\sqrt{6}}$	$(\mathcal{B}' - \mathcal{B} + \mathcal{C} + \mathcal{C}' - \mathcal{E}_{u-c} - \mathcal{E}'_{u-c})$	$+ V_{td} V_{tb}^* \frac{1}{\sqrt{6}}$	$(-\mathcal{E}_{t-c} - \mathcal{E}'_{t-c})$	7.3×10^{-6}		
$\to \rho^0 \eta'$	$V_{ud} V_{ub}^* \frac{1}{2\sqrt{3}}$	$(\mathcal{B}' - \mathcal{B} + \mathcal{C} + \mathcal{C}' - \mathcal{E}_{u-c} - \mathcal{E}'_{u-c})$	$+ V_{td} V_{tb}^* \frac{1}{2\sqrt{3}}$	$(-\mathcal{E}_{t-c} - \mathcal{E}'_{t-c})$	1.2×10^{-5}		
$\to \omega \pi^0$	$V_{ud} V_{ub}^* \frac{1}{2}$	$(\mathcal{B} - \mathcal{B}' + \mathcal{C} + \mathcal{C}' - \mathcal{E}_{u-c} - \mathcal{E}'_{u-c})$	$+ V_{td} V_{tb}^* \frac{1}{2}$	$(-\mathcal{E}_{t-c} - \mathcal{E}'_{t-c})$	1.2×10^{-5}	4.6×10^{-4}	
$\to \omega \eta$	$V_{ud} V_{ub}^* \frac{1}{\sqrt{6}}$	$(\mathcal{B}' + \mathcal{B} + \mathcal{C} + \mathcal{C}' + \mathcal{E}_{u-c} + \mathcal{E}'_{u-c})$	$+ V_{td} V_{tb}^* \frac{1}{\sqrt{6}}$	$(\mathcal{E}_{t-c} + \mathcal{E}'_{t-c})$	4.7×10^{-6}		
$\to \omega \eta'$	$V_{ud} V_{ub}^* \frac{1}{2\sqrt{3}}$	$(\mathcal{B}' + \mathcal{B} + \mathcal{C} + \mathcal{C}' + \mathcal{E}_{u-c} + \mathcal{E}'_{u-c})$	$+ V_{td} V_{tb}^* \frac{1}{2\sqrt{3}}$	$(\mathcal{E}_{t-c} + \mathcal{E}'_{t-c})$	1.5×10^{-5}		
$\to \phi \eta$	$V_{ud} V_{ub}^* \frac{1}{\sqrt{3}}$	$(-\mathcal{F}_{u-c})$	$+ V_{td} V_{tb}^* \frac{1}{\sqrt{3}}$	$(-\mathcal{F}_{t-c})$			
$\to \phi \eta'$	$V_{ud} V_{ub}^* \frac{1}{\sqrt{6}}$	$(2\mathcal{F}_{u-c})$	$+ V_{td} V_{tb}^* \frac{1}{\sqrt{6}}$	$(2\mathcal{F}_{t-c})$			
$B_u^+ \to K^+ \rho^0$	$V_{us} V_{ub}^* \frac{1}{\sqrt{2}}$	$(\mathcal{A}' + \mathcal{B}' + \mathcal{D}' + \mathcal{E}_{u-c})$	$+ V_{ts} V_{tb}^* \frac{1}{\sqrt{2}}$	$(\mathcal{E}_{t-c})$	6.0×10^{-7}	1.8×10^{-4}	7.0×10^{-5}
$\to K^{*+} \pi^0$	$V_{us} V_{ub}^* \frac{1}{\sqrt{2}}$	$(\mathcal{A} + \mathcal{B} + \mathcal{D} + \mathcal{E}'_{u-c})$	$+ V_{ts} V_{tb}^* \frac{1}{\sqrt{2}}$	$(\mathcal{E}'_{t-c})$	8.9×10^{-6}		
$\to K^0 \rho^+$	$V_{us} V_{ub}^*$	$(\mathcal{D}' + \mathcal{E}_{u-c})$	$+ V_{ts} V_{tb}^*$	$(\mathcal{E}_{t-c})$	3.4×10^{-7}		
$\to K^{*0} \pi^+$	$V_{us} V_{ub}^*$	$(\mathcal{D} + \mathcal{E}'_{u-c})$	$+ V_{ts} V_{tb}^*$	$(\mathcal{E}'_{t-c})$	8.8×10^{-6}	1.7×10^{-4}	1.3×10^{-4}
$\to K^+ \phi$	$V_{us} V_{ub}^*$	$(\mathcal{D} + \mathcal{E}'_{u-c})$	$+ V_{ts} V_{tb}^*$	$(\mathcal{E}'_{t-c})$	1.4×10^{-5}	1.8×10^{-4}	8.0×10^{-5}
$\to K^+ \omega$	$V_{us} V_{ub}^* \frac{1}{\sqrt{2}}$	$(\mathcal{A}' + \mathcal{B}' + \mathcal{D}' + \mathcal{E}_{u-c})$	$+ V_{ts} V_{tb}^* \frac{1}{\sqrt{2}}$	$(\mathcal{E}_{t-c})$	1.4×10^{-6}		

TABLE III. (*Continued*).

Reaction	Amplitude			$(\mathrm{Br})_{\mathrm{theory}}$	Expt. limits from ARGUS	CLEO
$\to\rho^+\pi^0$	$V_{ud}V_{ub}^*\frac{1}{\sqrt{2}}$	$(\mathcal{A}+\mathcal{B}-\mathcal{C}_{u-c}+\mathcal{C}'_{u-c})$	$+V_{td}V_{tb}^*\frac{1}{\sqrt{2}}$	$(-\mathcal{C}_{t-c}+\mathcal{C}'_{t-c})$	1.7×10^{-5}	5.5×10^{-4}	
$\to\rho^0\pi^+$	$V_{ud}V_{ub}^*\frac{1}{\sqrt{2}}$	$(\mathcal{A}'+\mathcal{B}'+\mathcal{C}_{u-c}-\mathcal{C}'_{u-c})$	$+V_{td}V_{tb}^*\frac{1}{\sqrt{2}}$	$(\mathcal{C}_{t-c}-\mathcal{C}'_{t-c})$	3.7×10^{-6}	1.5×10^{-4}	1.5×10^{-4}
$\to\omega\pi^+$	$V_{ud}V_{ub}^*\frac{1}{\sqrt{2}}$	$(\mathcal{A}'+\mathcal{B}'+2\mathcal{D}'+\mathcal{C}_{u-e}+\mathcal{C}'_{u-c})$	$+V_{td}V_{tb}^*\frac{1}{\sqrt{2}}$	$(\mathcal{C}_{t-c}+\mathcal{C}'_{t-c})$	4.7×10^{-6}	4.0×10^{-4}	
$\to K^{*+}\bar{K}^0$	$V_{ud}V_{qb}^*$	$(\mathcal{D}'+\mathcal{C}_{u-c})$	$+V_{td}V_{td}^*$	$(\mathcal{C}_{t-c})$	3.9×10^{-8}		
$\to K^+\bar{K}^{*0}$	$V_{ud}V_{qb}^*$	$(\mathcal{D}+\mathcal{C}'_{u-c})$	$+V_{td}V_{tb}^*$	$(\mathcal{C}'_{t-c})$	1.0×10^{-6}		
$\to K^{*+}\eta$	$V_{us}V_{ub}^*\frac{1}{\sqrt{3}}$	$(\mathcal{A}+\mathcal{B}-\mathcal{C}_{u-c}+\mathcal{C}'_{u-c})$	$+V_{ts}V_{tb}^*\frac{1}{\sqrt{3}}$	$(-\mathcal{C}_{t-c}+\mathcal{C}'_{t-c})$	1.2×10^{-5}		
$-K^{*+}\eta'$	$V_{us}V_{ub}^*\frac{1}{\sqrt{6}}$	$(\mathcal{A}+\mathcal{B}+3\mathcal{D}+2\mathcal{C}_{u-c}+\mathcal{C}'_{u-c})$	$+V_{ts}V_{tb}^*\frac{1}{\sqrt{6}}$	$(2\mathcal{C}_{t-c}+\mathcal{C}'_{t-c})$	8.1×10^{-6}		
$\to\rho^+\eta$	$V_{ud}V_{qb}^*\frac{1}{\sqrt{3}}$	$(\mathcal{A}+\mathcal{B}+2\mathcal{D}+\mathcal{C}_{u-c}+\mathcal{C}'_{u-c})$	$+V_{td}V_{tb}^*\frac{1}{\sqrt{3}}$	$(\mathcal{C}_{t-c}+\mathcal{C}'_{t-c})$	4.3×10^{-5}		
$\to\rho^+\eta'$	$V_{ud}V_{qb}^*\frac{1}{\sqrt{6}}$	$(\mathcal{A}+\mathcal{B}+2\mathcal{D}+\mathcal{C}_{u-c}+\mathcal{C}'_{u-c})$	$+V_{td}V_{tb}^*\frac{1}{\sqrt{6}}$	$(\mathcal{C}_{t-c}+\mathcal{C}'_{t-c})$	5.3×10^{-5}		

(ii) Decay modes in which both the spectator and W-loop (penguin) contributions are comparable, e.g., $B_u^+\to K^+\pi^0, K^{*+}\pi^0, K^+\rho^0, K^+\omega, \ldots$; $B_d^0\to K^+\pi^-$, $K^+\rho^-, \ldots$. In addition to the W-loop diagram, those channels can also proceed through the external W-emission mechanism $\mathcal{A}$. Although the loop-induced amplitude $\mathcal{E}$ is typically suppressed by a factor of $\alpha_s/4\pi$, it does not suffer from Cabibbo double suppression encountered by the spectator diagram. As a result of this tradeoff, one has $O(V_{us}V_{ub}^*\mathcal{A})\sim O(V_{cs}V_{cb}^*\mathcal{E})$ in general.

(iii) Decay modes dominated by the spectator diagram. Decays such as $B_u^+\to\pi^+\omega, \rho^+\pi^0, \rho^0\pi^+, \ldots$, $B_d^0\to\pi^+\pi^-, \rho^+\pi^-, \pi^+\rho^-, \eta\eta, \pi^0\omega, \ldots$, fall into this category. The KM matrix elements $V_{ud}V_{ub}^*$ associated with the spectator amplitude $\mathcal{A}$ are of the same order of magnitude as $V_{cd}V_{cb}^*$ and $V_{td}V_{tb}^*$. Therefore, one will generally have $|V_{ud}V_{ub}^*\mathcal{A}| \gg |V_{cd}V_{cb}^*\mathcal{E}|$ in this case.

We see that W-loop diagrams play a crucial role in rare B decays. The quark-diagram scheme, in addition to being helpful in organizing our theoretical calculations, can be used to analyze experimental data directly, as we are going to discuss shortly. When enough measurements are made on charmless B decays, we can find out the values of each quark-diagram amplitude from experiment and compare to our theoretical results given here, especially checking whether there are any final-state interactions or whether the W-annihilation and the W-exchange diagrams can be ignored. Note that some of decays are purely from W-loop diagrams[14] and hence their comparison with experiments can give direct values of the amplitudes which can then be used to compare with the penguin calculations given here. Also, note that $B^+\to\pi^+\pi^0, \rho^+\rho^0$ can happen only via nonvanishing $|V_{ub}|$. Thus their observation will provide an unambiguous proof of $|V_{ub}|\neq 0$.

The horizontal W-loop diagram $\mathcal{E}$ can be determined directly from the decay modes $B_d^0\to K^0\phi$ and $K^*\phi$, while the vertical W-loop diagram $\mathcal{F}$ can be extracted from $B_d^0\to\phi\phi$, $\phi\eta$, and $\phi\eta'$. The relative sign of $\mathcal{E}$ and $\mathcal{F}$ is fixed by the measurement of $B_d^0\to K^0\bar{K}^0, K^0\bar{K}^{0*}, \ldots$.

In the absence of final-state interactions, the internal W-emission amplitude $\mathcal{B}$ is measured from $B_d^0\to K^0\pi^0, K^0\rho^0, K^{*0}\pi^0, K^0\omega, \ldots$. By the same token, we can find the magnitude of $\mathcal{A}$ from $B_d^0\to K^+\pi^-, K^+\rho^-, \ldots$. The decays $B_u^+\to\pi^+\pi^0, \rho^+\rho^0$ can then be utilized to determine the relative sign of $\mathcal{A}$ and $\mathcal{B}$. As we stressed before, these two channels depend solely on $V_{ud}^*V_{ub}$: that is, they can occur only via nonvanishing $|V_{ub}|$.

Once the horizontal W-loop amplitude is known, it is straightforward to extract the information on W-annihilation $\mathcal{D}$ from $B_u^+\to K^0\pi^+, K^+\bar{K}^0, K^0\rho^+, K^{*0}\pi^+, K^+\phi$. The determination of W-exchange $\mathcal{C}$ is somewhat indirect: it requires the knowledge of $\mathcal{A}$ (or $\mathcal{B}$), $\mathcal{E}$ and $\mathcal{F}$ in the decays $B_d^0\to\pi^+\pi^-, \pi^0\pi^0$. Then we can see if $\mathcal{C}$ and $\mathcal{D}$ are really important.

We have demonstrated above the use of this scheme for determining the quark-diagram amplitudes. In the following we present a few explicit examples of model calculations for illustrative purposes.

TABLE IV. Same as Table II, for $B \to VV$ decays.

Reaction	Amplitude				$(\mathrm{Br})_{\mathrm{theory}}$	Expt. limits from ARGUS	Expt. limits from CLEO
$B_d^0 \to K^{*+}\rho^-$	$V_{us}V_{ub}^*$	$(\mathcal{A}+\mathcal{E}_{u-c})$	$+V_{ts}V_{tb}^*$	$(\mathcal{E}_{t-c})$	1.8×10^{-5}		
$\to K^{*0}\bar{K}^{*0}$	$V_{ud}V_{ub}^*$	$(\mathcal{E}_{u-c}+\mathcal{F}_{u-c})$	$+V_{td}V_{tb}^*$	$(\mathcal{E}_{t-c}+\mathcal{F}_{t-c})$	9.6×10^{-7}		
$\to K^{*0}\rho^0$	$V_{us}V_{ub}^*\frac{1}{\sqrt{2}}$	$(\mathcal{B}-\mathcal{E}_{u-c})$	$+V_{ts}V_{tb}^*\frac{1}{\sqrt{2}}$	$(-\mathcal{E}_{t-c})$	4.7×10^{-6}	4.6×10^{-4}	6.7×10^{-4}
$\to K^{*0}\phi$	$V_{us}V_{ub}^*$	$(\mathcal{E}_{u-c})$	$+V_{ts}V_{tb}^*$	$(\mathcal{E}_{t-c})$	9.0×10^{-6}	3.2×10^{-4}	4.4×10^{-4}
$\to K^{*0}\omega$	$V_{us}V_{ub}^*\frac{1}{\sqrt{2}}$	$(\mathcal{B}+\mathcal{E}_{u-c})$	$+V_{ts}V_{tb}^*\frac{1}{\sqrt{2}}$	$(\mathcal{E}_{t-c})$	8.1×10^{-6}		
$\to \rho^+\rho^-$	$V_{ud}V_{ub}^*$	$(\mathcal{A}+\mathcal{C}+\mathcal{E}_{u-c}+\mathcal{F}_{u-c})$	$+V_{td}V_{tb}^*$	$(\mathcal{E}_{t-c}+\mathcal{F}_{t-c})$	3.4×10^{-5}	2.2×10^{-3}	
$\to \rho^0\rho^0$	$V_{ud}V_{ub}^*\frac{1}{2}$	$(-\mathcal{B}+\mathcal{C}+\mathcal{E}_{u-c}+\mathcal{F}_{u-c})$	$+V_{td}V_{tb}^*\frac{1}{2}$	$(\mathcal{E}_{t-c}+\mathcal{F}_{t-c})$	1.6×10^{-6}	2.8×10^{-4}	3.4×10^{-4}
$\to \rho^0\omega$	$V_{ud}V_{ub}^*\frac{1}{2}$	$(-\mathcal{B}+\mathcal{B}'-\mathcal{E}_{u-c}-\mathcal{E}'_{u-c})$	$+V_{td}V_{tb}^*\frac{1}{2}$	$(-\mathcal{E}_{t-c}-\mathcal{E}'_{t-c})$	3.9×10^{-7}		
$\to \omega\omega$	$V_{ud}V_{ub}^*\frac{1}{2}$	$(\mathcal{B}+\mathcal{C}+\mathcal{E}_{u-c}+\mathcal{F}_{u-c})$	$+V_{td}V_{tb}^*\frac{1}{2}$	$(\mathcal{E}_{t-c}+\mathcal{F}_{t-c})$	2.8×10^{-6}		
$\to \phi\phi$	$V_{ud}V_{ub}^*$	$(\mathcal{F}_{u-c})$	$+V_{td}V_{tb}^*$	$(\mathcal{F}_{t-c})$			
$B_u^+ \to K^{*+}\rho^0$	$V_{us}V_{ub}^*\frac{1}{\sqrt{2}}$	$(\mathcal{A}+\mathcal{B}+\mathcal{D}+\mathcal{E}_{u-c})$	$+V_{ts}V_{tb}^*\frac{1}{\sqrt{2}}$	$(\mathcal{E}_{t-c})$	7.6×10^{-6}		
$\to K^{0*}\rho^+$	$V_{us}V_{ub}^*$	$(\mathcal{D}+\mathcal{E}_{u-c})$	$+V_{ts}V_{tb}^*$	$(\mathcal{E}_{t-c})$	8.0×10^{-6}	9.0×10^{-4}	
$\to K^{*+}\phi$	$V_{us}V_{ub}^*$	$(\mathcal{D}+\mathcal{E}_{u-c})$	$+V_{ts}V_{tb}^*$	$(\mathcal{E}_{t-c})$	8.2×10^{-6}		
$\to K^{*+}\omega$	$V_{us}V_{ub}^*\frac{1}{\sqrt{2}}$	$(\mathcal{A}+\mathcal{B}+\mathcal{D}+\mathcal{E}_{u-c})$	$+V_{ts}V_{tb}^*\frac{1}{\sqrt{2}}$	$(\mathcal{E}_{t-c})$	1.5×10^{-5}	1.3×10^{-4}	
$\to K^{*+}\bar{K}^{*0}$	$V_{ud}V_{ub}^*$	$(\mathcal{D}+\mathcal{E}_{u-c})$	$+V_{td}V_{tb}^*$	$(\mathcal{E}_{t-c})$	1.0×10^{-6}		
$\to \rho^+\rho^0$	$V_{ud}V_{ub}^*\frac{1}{\sqrt{2}}$	$(\mathcal{A}+\mathcal{B})$			1.4×10^{-5}	1.0×10^{-3}	
$\to \rho^+\omega$	$V_{ud}V_{ub}^*\frac{1}{\sqrt{2}}$	$(\mathcal{A}+\mathcal{B}+2\mathcal{D}+\mathcal{E}_{u-c}+\mathcal{E}'_{u-c})$	$+V_{td}V_{tb}^*\frac{1}{\sqrt{2}}$	$(\mathcal{E}_{t-c}+\mathcal{E}'_{t-c})$	2.5×10^{-5}		

TABLE V. Same as Table II, for $B \to PA$ decays.

Reaction	Amplitude				$(\mathrm{Br})_{\mathrm{theory}}$	Expt. limits from ARGUS	Expt. limits from CLEO
$B_d^0 \to K^+ a_1^-$	$V_{us}V_{ub}^*$	$(\mathcal{A}+\mathcal{E}_{u-c})$	$+V_{ts}V_{tb}^*$	$(\mathcal{E}_{t-c})$			
$\to K^0 a_1^0$	$V_{us}V_{ub}^*\frac{1}{\sqrt{2}}$	$(\mathcal{B}+\mathcal{E}_{u-c})$	$+V_{ts}V_{tb}^*\frac{1}{\sqrt{2}}$	$(\mathcal{E}_{t-c})$			
$\to \pi^+ a_1^-$	$V_{ud}V_{ub}^*$	$(\mathcal{A}+\mathcal{C}+\mathcal{E}_{u-c}+\underline{\mathcal{E}}_{u-c}+\mathcal{T}_{u-c})$	$+V_{td}V_{tb}^*$	$(\mathcal{E}_{t-c}+\underline{\mathcal{E}}_{t-c}+\mathcal{T}_{t-c})$		6.3×10^{-4}	5.7×10^{-4}
$\to \pi^- a_1^+$	$V_{ud}V_{ub}^*$	$(\mathcal{A}+\mathcal{C}+\mathcal{E}_{u-c}+\underline{\mathcal{E}}_{u-c}+\mathcal{T}_{u-c})$	$+V_{td}V_{tb}^*$	$(\mathcal{E}_{t-c}+\underline{\mathcal{E}}_{t-c}+\mathcal{T}_{t-c})$			5.7×10^{-4}
$\to \pi^0 a_1^0$	$V_{ud}V_{ub}^*\frac{1}{2}$	$(-\underline{\mathcal{B}}-\mathcal{B}+\mathcal{C}+\mathcal{E}_{u-c}+\underline{\mathcal{E}}_{u-c}+\mathcal{T}_{u-c})$	$+V_{td}V_{tb}^*\frac{1}{2}$	$(\mathcal{E}_{t-c}+\underline{\mathcal{E}}_{t-c}+\mathcal{T}_{t-c})$		1.1×10^{-3}	
$\to \eta a_1^0$	$V_{ud}V_{ub}^*\frac{1}{\sqrt{6}}$	$(-\mathcal{B}+\underline{\mathcal{B}}+\mathcal{C}-\mathcal{E}_{u-c}-\underline{\mathcal{E}}_{u-c})$	$+V_{td}V_{tb}^*\frac{1}{\sqrt{6}}$	$(-\mathcal{E}_{t-c}-\underline{\mathcal{E}}_{t-c})$			
$\to \eta' a_1^0$	$V_{ud}V_{ub}^*\frac{1}{2\sqrt{3}}$	$(-\mathcal{B}+\underline{\mathcal{B}}+\mathcal{C}-\mathcal{E}_{u-c}-\underline{\mathcal{E}}_{u-c})$	$+V_{td}V_{tb}^*\frac{1}{2\sqrt{3}}$	$(-\mathcal{E}_{t-c}-\underline{\mathcal{E}}_{t-c})$			
$B_u^+ \to \pi^0 a_1^+$	$V_{ud}V_{ub}^*\frac{1}{\sqrt{2}}$	$(\mathcal{A}+\mathcal{B}-\mathcal{E}_{u-c}+\mathcal{E}'_{u-c})$	$+V_{td}V_{tb}^*\frac{1}{\sqrt{2}}$	$(-\mathcal{E}_{t-c}+\mathcal{E}'_{t-c})$		1.7×10^{-3}	
$\to \pi^+ a_1^0$	$V_{ud}V_{ub}^*\frac{1}{\sqrt{2}}$	$(\mathcal{A}'+\mathcal{B}'+\mathcal{E}_{u-c}-\mathcal{E}'_{u-c})$	$+V_{td}V_{tb}^*\frac{1}{\sqrt{2}}$	$(\mathcal{E}_{t-c}-\mathcal{E}'_{t-c})$		9.0×10^{-4}	
$\to K^0 a_1^+$	$V_{us}V_{ub}^*$	$(\mathcal{D}+\mathcal{E}_{u-c})$	$+V_{ts}V_{tb}^*$	$(\mathcal{E}_{t-c})$			
$\to K^+ a_1^0$	$V_{us}V_{ub}^*\frac{1}{\sqrt{2}}$	$(\mathcal{A}+\mathcal{B}+\mathcal{D}+\mathcal{E}_{u-c})$	$+V_{ts}V_{tb}^*\frac{1}{\sqrt{2}}$	$(\mathcal{E}_{t-c})$			
$\to \eta a_1^+$	$V_{ud}V_{ub}^*\frac{1}{\sqrt{3}}$	$(\mathcal{A}+\mathcal{B}+2\mathcal{D}+\mathcal{E}_{u-c}+\mathcal{E}'_{u-c})$	$+V_{td}V_{tb}^*\frac{1}{\sqrt{3}}$	$(\mathcal{E}_{t-c}+\mathcal{E}'_{t-c})$			
$\to \eta' a_1^+$	$V_{ud}V_{ub}^*\frac{1}{\sqrt{6}}$	$(\mathcal{A}+\mathcal{B}+2\mathcal{D}+\mathcal{E}_{u-c}+\mathcal{E}'_{u-c})$	$+V_{td}V_{tb}^*\frac{1}{\sqrt{6}}$	$(\mathcal{E}_{t-c}+\mathcal{E}'_{t-c})$			

TABLE VI. Same as Table II, for $B \to VA$ decays.

Reaction	Amplitude				$(\mathrm{Br})_{\mathrm{theory}}$	Expt. limits from ARGUS	CLEO
$B_d^0 \to K^{*+} a_1^-$	$V_{us}V_{ub}^*$	$(\mathcal{A}+\mathcal{E}_{u-c})$	$+V_{ts}V_{tb}^*$	$(\mathcal{E}_{t-c})$			
$\to K^{*0} a_1^0$	$V_{us}V_{ub}^*\frac{1}{\sqrt{2}}$	$(\mathcal{B}+\mathcal{E}_{u-c})$	$+V_{ts}V_{tb}^*\frac{1}{\sqrt{2}}$	$(\mathcal{E}_{t-c})$			
$\to \rho^+ a_1^-$	$V_{ud}V_{ub}^*$	$(\mathcal{A}'+\mathcal{C}+\mathcal{E}_{u-c}+\mathcal{E}'_{u-c}+\mathcal{T}_{u-c})$	$+V_{td}V_{tb}^*$	$(\mathcal{E}_{t-c}+\mathcal{E}'_{t-c}+\mathcal{T}_{t-c})$			
$\to \rho^- a_1^+$	$V_{ud}V_{ub}^*$	$(\mathcal{A}+\mathcal{C}'+\mathcal{E}_{u-c}+\mathcal{E}'_{u-c}+\mathcal{T}_{u-c})$	$+V_{td}V_{tb}^*$	$(\mathcal{E}_{t-c}+\mathcal{E}'_{t-c}+\mathcal{T}_{t-c})$		3.4×10^{-3}	
$\to \rho^0 a_1^0$	$V_{ud}V_{ub}^*\frac{1}{2}$	$(-\mathcal{B}'-\mathcal{B}+\mathcal{C}+\mathcal{E}_{u-c}+\mathcal{E}'_{u-c}+\mathcal{T}_{u-c})$	$+V_{td}V_{tb}^*\frac{1}{2}$	$(\mathcal{E}_{t-c}+\mathcal{E}'_{t-c}+\mathcal{T}_{t-c})$		2.4×10^{-3}	
$\to \omega a_1^0$	$V_{ud}V_{ub}^*\frac{1}{2}$	$(-\mathcal{B}'+\mathcal{B}+\mathcal{C}-\mathcal{E}_{u-c}-\mathcal{E}'_{u-c})$	$+V_{td}V_{tb}^*\frac{1}{2}$	$(-\mathcal{E}_{t-c}-\mathcal{E}'_{t-c})$			
$B_u^+ \to \rho^0 a_1^+$	$V_{ud}V_{ub}^*\frac{1}{\sqrt{2}}$	$(\mathcal{A}+\mathcal{B}+\mathcal{E}_{u-c}-\mathcal{E}'_{u-c})$	$+V_{td}V_{tb}^*\frac{1}{\sqrt{2}}$	$(\mathcal{E}_{t-c}-\mathcal{E}'_{t-c})$		6.0×10^{-4}	5.4×10^{-4}
$\to \rho^+ a_1^0$	$V_{ud}V_{ub}^*\frac{1}{\sqrt{2}}$	$(\mathcal{A}+\mathcal{B}+\mathcal{E}_{u-c})$	$+V_{td}V_{tb}^*\frac{1}{\sqrt{2}}$	$(\mathcal{E}_{t-c})$			
$\to \omega a_1^+$	$V_{ud}V_{ub}^*\frac{1}{\sqrt{2}}$	$(\mathcal{A}+\mathcal{B}+2\mathcal{D}+\mathcal{E}_{u-c}+\mathcal{E}'_{u-c})$	$+V_{td}V_{tb}^*\frac{1}{\sqrt{2}}$	$(\mathcal{E}_{t-c}+\mathcal{E}'_{t-c})$			
$\to K^{*0} a_1^+$	$V_{us}V_{ub}^*$	$(\mathcal{D}+\mathcal{E}_{u-c})$	$+V_{ts}V_{tb}^*$	$(\mathcal{E}_{t-c})$			
$\to K^{*+} a_1^0$	$V_{us}V_{ub}^*\frac{1}{\sqrt{2}}$	$(\mathcal{A}+\mathcal{B}+\mathcal{D}+\mathcal{E}_{u-c})$	$+V_{ts}V_{tb}^*\frac{1}{\sqrt{2}}$	$(\mathcal{E}_{t-c})$			

TABLE VII. Same as Table II, for $B \to AA$ decays.

Reaction	Amplitude				$(\mathrm{Br})_{\mathrm{theory}}$	Expt. limits from ARGUS	CLEO
$B_d^0 \to a_1^0 a_1^0$	$V_{ud}V_{ub}^*\frac{1}{2}$	$(-\mathcal{B}+\mathcal{C}+\mathcal{E}_{u-c}+\mathcal{T}_{u-c})$	$+V_{td}V_{tb}^*\frac{1}{2}$	$(\mathcal{E}_{t-c}+\mathcal{T}_{t-c})$			
$\to a_1^+ a_1^-$	$V_{ud}V_{ub}^*$	$(\mathcal{A}+\mathcal{C}+\mathcal{E}_{u-c}+\mathcal{T}_{u-c})$	$+V_{td}V_{tb}^*$	$(\mathcal{E}_{t-c}+\mathcal{T}_{t-c})$		6.0×10^{-3}	3.2×10^{-3}
$B_u^+ \to a_1^0 a_1^+$	$V_{ud}V_{ub}^*\frac{1}{\sqrt{2}}$	$(\mathcal{A}+\mathcal{B})$					

IV. MODEL CALCULATIONS

A. The decay $B \to PP$

A simple and widely employed approach for evaluating the nonleptonic weak decay amplitude of mesons is based on the valence-quark assumption and vacuum-insertion approximation in which the matrix elements of two quark bilinear operators are saturated by the vacuum intermediate states in all possible ways.[2] This factorization method, when applied to heavy meson decay, fails to explain color-suppressed decay modes. This difficulty calls for the necessity of modification.[2] As explained in Sec. II B and Appendix A, we will treat the common QCD-corrected factor $(2c_+ - c_-)/3$ for color-mismatched decay as a free parameter. A fit to data requires it be ≈ -0.25 [Eq. (A7)]. For $(c_+ + c_-)/3$, we take it to be the usual QCD-corrected value, namely, ≈ 1.04.

As an example for $B \to PP$ decay, we consider $B_u^+ \to K^0 \pi^+$. Its quark-diagram amplitude is given by

$$A(B_u^+ \to K^0 \pi^+) = \lambda_u(\mathcal{D} + \mathcal{E}_{u-c}) + \lambda_t(\mathcal{E}_{t-c}) , \quad (4.1)$$

where $\lambda_i \equiv V_{is} V_{ib}^*$, $\mathcal{E}_{u-c} \equiv \mathcal{E}_u - \mathcal{E}_c$, $\mathcal{E}_{t-c} \equiv \mathcal{E}_t - \mathcal{E}_c$. The penguin amplitude consists of two contributions—one from the timelike penguin diagram and the other from the spacelike configuration:

$$\mathcal{E}_i = \langle K^0 \pi^+ | H_{\text{peng}} | B_u^+ \rangle_i = \frac{G_F}{\sqrt{2}} \frac{\alpha_s}{\pi} \left[I_i^{\text{time}} \left[1 + 2 \frac{m_K^2}{(m_s + m_d)(m_b - m_d)} \right] F_t + I_i^{\text{space}} \left[1 + 2 \frac{m_B^2}{(m_b + m_u)(m_s - m_u)} \right] F_s \right] , \quad (4.2)$$

with

$$F_t = \langle K^0 | (\bar{s}d) | 0 \rangle \langle \pi^+ | (\bar{d}b) | B_u^+ \rangle , \quad (4.3)$$

$$F_s = \langle K^0 \pi^+ | (\bar{s}u) | 0 \rangle \langle 0 | (\bar{u}b) | B_u^+ \rangle ,$$

where $(\bar{q}_1 q_2) = \bar{q}_1 \gamma_\mu (1 - \gamma_5) q_2$, and uses of the equations of motion have been made

$$-i\partial^\mu (\bar{q}_1 \gamma_\mu \gamma_5 q_2) = (m_1 + m_2) \bar{q}_1 \gamma_5 q_2 , \quad (4.4)$$

$$-i\partial^\mu (\bar{q}_1 \gamma_\mu q_2) = (m_1 - m_2) \bar{q}_1 q_2 .$$

From Eqs. (2.17) and (2.19) it turns out

$$F_t = i f_K \frac{m_B - m_\pi}{m_B + m_\pi} [(m_B + m_\pi)^2 - m_K^2] f_+^{B\pi}(m_K^2) , \quad (4.5)$$

$$F_s = -i f_{B_u} \frac{m_K - m_\pi}{m_K + m_\pi} [(m_K + m_\pi)^2 - m_B^2] f_+^a(m_B^2) .$$

The annihilation diagram F_s is expected to be suppressed in the case of rare B decay for two arguments. First, the reaction $b\bar{q} \to s\bar{q}$ $(q = u,d,s)$ is helicity suppressed.[31] Second, in the annihilation process we are considering a decay of a very heavy object into two very light quarks. Since these two quarks are very energetic, it is difficult for them to have enough time to perform hadronization. Indeed, using $f_+^{BK}(0) = 0.38$ and $f_+^a(q^2) = i 16\pi \alpha_s f^2 / q^2$ of Ref. 32 for the annihilation form factor, we find numerically

$$F_s = i 1.2 \times 10^{-2} F_t . \quad (4.6)$$

Upon a close look, Eq. (4.2) exhibits however an interesting feature: the annihilation contribution to the spacelike penguin diagram is enhanced by a factor of m_B^2/m_K^2. This means that the spacelike penguin amplitude is primarily absorptive and is not negligible *a priori*.

Choosing $m_t = 100$ GeV, and $|k^2| = m_b^2/2$, it follows from Table I that

$$\begin{aligned} (I_t - I_c)_{\text{time}} &= 1.238 + i 0.383 , \\ (I_t - I_c)_{\text{space}} &= 0.961 , \\ (I_u - I_c)_{\text{time}} &= 0.264 - i 0.140 , \\ (I_u - I_c)_{\text{space}} &= -0.113 . \end{aligned} \quad (4.7)$$

This leads to

$$A(B_u^+ \to K^0 \pi^+) = i \frac{G_F}{\sqrt{2}} [\lambda_u (1.24 + i 0.22) + \lambda_t (5.83 + i 4.24)] \times 10^{-2} F_t , \quad (4.8)$$

The decay rate is then given by

$$\Gamma(B_u^+ \to K^0 \pi^+) = \frac{p_c}{8\pi m_B^2} |A|^2 , \quad (4.9)$$

where p_c is the c.m. momentum of the final-state particle

$$p_c = \frac{\{[m_B^2 - (m_{K^*} + m_\omega)^2][m_B^2 - (m_{K^*} - m_\omega)^2]\}^{1/2}}{2m_B} . \quad (4.10)$$

The branching ratio turns out to be

$$B(B_u^+ \to K^0 \pi^+) = 1.2 \times 10^{-5} \quad (4.11)$$

for $\tau_B = 1.2 \times 10^{-12}$ sec. In Sec. IV E, we will discuss the dependence of the branching ratio on k^2 and m_t.

B. The decay $B \to VP$

The example we wish to demonstrate is $B_u^+ \to K^+ \rho^0$, whose quark-diagram amplitude reads

$$A(B_u^+ \to K^+ \rho^0) = \frac{1}{\sqrt{2}} \lambda_u (\mathcal{A}' + \mathcal{B}' + \mathcal{D}' + \mathcal{E}_{u-c}) + \frac{1}{\sqrt{2}} \lambda_t (\mathcal{E}_{t-c}) , \quad (4.12)$$

where the primed amplitude denotes the case that the vector meson arises from the decay of the b quark. [We define $\mathcal{D}'$ $(\mathcal{D})$ for the W-annihilation amplitude if the vector meson comes from q_1 $(\bar{q}_2)$.] In the vacuum-insertion approximation, one obtains

$$\mathcal{A}'=c_1 G_F\langle K^+|(\bar{s}u)|0\rangle\langle\rho^0|(\bar{u}b)|B_u^+\rangle\ ,$$
$$\mathcal{B}'=c_2 G_F\langle\rho^0|(\bar{u}u)|0\rangle\langle K^+|(\bar{s}b)|B_u^+\rangle\ , \tag{4.13}$$
$$\mathcal{D}'=c_1 G_F\langle K^+\rho^0|(\bar{s}u)|0\rangle\langle 0|(\bar{u}b)|B_u^+\rangle\ ;$$

and

$$\mathcal{E}_i=\frac{\alpha_s}{\pi}\frac{4}{9}\left[I_i^{\rm time}\left[1-2\frac{m_K^2}{(m_s+m_u)(m_b+m_u)}\right]\tilde{\mathcal{A}}'+I_i^{\rm space}\left[1-2\frac{m_B^2}{(m_s+m_u)(m_b+m_u)}\right]\tilde{\mathcal{D}}'\right], \tag{4.14}$$

where $c_1=(2c_+ +c_-)/3$, $c_2=(2c_+ -c_-)/3$, $\mathcal{A}'=c_1\tilde{\mathcal{A}}'$, $\mathcal{D}'=c_1\tilde{\mathcal{D}}'$. We notice that the interference between $(V-A)(V+A)$ and $(S+P)(S-P)$ amplitudes in the penguin diagram of $B\to VP$ is destructive, while such interference in $B\to PP$ is constructive.

Applying the form factors given in Sec. II B leads to

$$\mathcal{A}'=c_1 G_F f_K[(m_B+m_\rho)A_1^{B\rho}(m_K^2)-(m_B-m_\rho)A_2^{B\rho}(m_K^2)](\epsilon\cdot p_B)\ ,$$
$$\mathcal{B}'=2c_2 G_F m_\rho^2 f_{\rho^0} f_+^{BK}(m_\rho^2)(\epsilon\cdot p_B)\ , \tag{4.15}$$
$$\mathcal{D}'=c_1 G_F f_{B_u}\left[(m_K+m_\rho)A_1^q(m_B^2)+\frac{m_B^2}{m_K+m_\rho}A_2^q(m_B^2)\right](\epsilon\cdot p_B)\ .$$

Unfortunately, we do not know at this point what are the annihilation form factors A_1^q and A_2^q at $q^2=m_B^2$. As stressed in the previous section, though the annihilation amplitude can be argued to be negligible compared to the external W-emission diagram, its contribution to the spacelike penguin diagram is enhanced by a factor of m_B^2/m_K^2 and should not be ignored *a priori*. Without further information on $\mathcal{D}'$, we shall however neglect the spacelike penguin contribution in our computations for $B\to VP$ rare decays. However, we shall keep this in mind when we compare these results with experiment. Since the annihilation penguin diagram is primarily absorptive, we believe that the theoretical uncertainties in the estimate of decay rates are at most of factors of 2 to 3 in either direction. Putting all results together, we get, for $|k^2|=m_B^2/2$,

$$A(B_u^+\to K^+\rho^0)=\frac{1}{\sqrt{2}}\lambda_u(0.66\tilde{\mathcal{A}}')+\frac{1}{\sqrt{2}}\lambda_t(1.21+i0.38)\times 10^{-2}\tilde{\mathcal{A}}'\ , \tag{4.16}$$

where uses have been made of $h_+^{BK}=0.379$, $h_{A_1}^{B\rho}=h_{A_2}^{B\rho}=0.283$. Since $|\lambda_u/\lambda_t|\approx 2.3\times 10^{-2}$, we see that spectator and penguin contributions are comparable. Because the polarization of ρ^0 is longitudinal, we obtain from (4.16) the branching ratio

$$B(B_u^+\to K^+\rho^0)=6.0\times 10^{-7}\ . \tag{4.17}$$

C. The decay $B\to VV$

To illustrate the calculation we focus on the decay mode $B_u^+\to K^{*+}\omega$, which has the quark-diagram amplitude

$$A(B_u^+\to K^{*+}\omega)=\frac{1}{\sqrt{2}}\lambda_u(\mathcal{A}+\mathcal{B}+\mathcal{D}+\mathcal{E}_{u-c})+\frac{1}{\sqrt{2}}\lambda_t(\mathcal{E}_{t-c})\ , \tag{4.18}$$

with

$$\mathcal{A}=c_1 G_F\langle K^{*+}|(\bar{s}u)|0\rangle\langle\omega|(\bar{u}b)|B_u^+\rangle\ ,$$
$$\mathcal{B}=c_2 G_F\langle\omega|(\bar{u}u)|0\rangle\langle K^{*+}|(\bar{s}b)|B_u^+\rangle\ ,$$
$$\mathcal{D}=c_1 G_F\langle K^{*+}\omega|(\bar{s}u)|0\rangle\langle 0|(\bar{u}b)|B_u^+\rangle\ , \tag{4.19}$$
$$\mathcal{E}_i=\frac{\alpha_s}{\pi}\frac{4}{9}(I_i^{\rm time}\tilde{\mathcal{A}}+I_i^{\rm space}\tilde{\mathcal{D}})\ .$$

It is noteworthy that there is no $(S+P)(S-P)$ contribution to the penguin amplitude for $B\to VV$ because of the constraint $\langle V|\bar{q}_L q_R'|0\rangle=0$. This means that the spacelike penguin diagram in this case can be safely neglected, contrary to $B\to VP$ decay.

It follows from Eqs. (2.14) and (2.21) that the quark-diagram amplitudes given by (4.19) can be recast into the form

$$-i\epsilon^\mu(K^*)\epsilon^\nu(\omega)(\hat{A}_1 g_{\mu\nu}+\hat{A}_2 p_\mu^B p_\nu^B+i\hat{B}\epsilon_{\mu\nu\alpha\beta}p_B^\alpha p_\omega^\beta)\ . \tag{4.20}$$

Unlike the $B\to VP$ case, the pseudoscalar-vector matrix element induced by the vector current does contribute to the decay amplitude of $B\to VV$. We obtain, for the external W-emission diagram $\mathcal{A}$,

$$\hat{A}_1=c_1 m_{K^*}^2 f_{K^*}(m_B+m_\omega)A_1^{B\omega}(m_{K^*}^2)\ ,$$
$$\hat{A}_2=-[2/(m_B+m_\omega)^2](h_{A_2}^{B\omega}/h_{A_1}^{B\omega})\hat{A}_1\ , \tag{4.21}$$
$$\hat{B}=(h_V^{B\omega}/h_{A_2}^{B\omega})\hat{A}_2\ ,$$

and, for the internal W-emission diagram $\mathcal{B}$,

$$\hat{A}_1=c_2 m_\omega^2 f_\omega(m_B+m_{K^*})A_1^{BK^*}(m_\omega^2)\ ,$$
$$\hat{A}_2=-[2/(m_B+m_{K^*})^2](h_{A_2}^{BK^*}/h_{A_1}^{BK^*})\hat{A}_1\ , \tag{4.22}$$
$$\hat{B}=(h_V^{BK^*}/h_{A_2}^{BK^*})\hat{A}_2\ .$$

Using the BSW estimation[5] for the form factors h_V, h_{A_1}, and h_{A_2}, we find numerically $\mathcal{B}\simeq -0.19\mathcal{A}$. The resulting decay amplitude is

$$A(B_u^+ \to K^{*+}\omega) = \frac{1}{\sqrt{2}}\lambda_u(0.81\mathcal{A}) + \frac{1}{\sqrt{2}}\lambda_t(3.74+i1.08)\times 10^{-2}\mathcal{A} \ . \tag{4.23}$$

It is convenient at this point to write the Lorentz-invariant amplitude $\mathcal{A}$ in terms of three helicity amplitudes:[21]

$$H_{00} = \frac{1}{m_{K^*}m_\omega}[\tfrac{1}{2}(m_B^2 - m_{K^*}^2 - m_\omega^2)\hat{A}_1 + m_B^2 p_c^2 \hat{A}_2] \ ,$$
$$H_{++} = \hat{A}_1 + m_B p_c \hat{B} \ , \tag{4.24}$$
$$H_{--} = \hat{A}_1 - m_B p_c \hat{B} \ ,$$

The decay rate is then given by

$$\Gamma(B_u^+ \to K^{*+}\omega) = \frac{p_c}{8\pi m_B^2}(|H_{00}|^2 + |H_{++}|^2 + |H_{--}|^2) \times |0.81\lambda_u + (3.74+i1.08)\times 10^{-2}\lambda_t|^2/2 \ , \tag{4.25}$$

which leads to the branching ratio

$$B(B_u^+ \to K^{*+}\omega) = 1.5\times 10^{-5} \ . \tag{4.26}$$

It is easily seen that $|H_{00}|^2 > |H_{--}|^2 > |H_{++}|^2$; i.e., the decay rate is dominated by the longitudinal helicity transition H_{00}. This pattern is indeed what is to be expected if factorization is a valid assumption.[33] Thus far, the ratio of $|H_{00}|^2/(|H_{++}|^2+|H_{--}|^2)$ has been tested only in the charmed decay $D \to \bar{K}^* \rho$.[22]

D. Results and discussion

The results of our calculations for the branching ratios of $B_u^+, B_d^0 \to PP, VP, VV$ are exhibited in Tables II–VII. Decay rates of exclusive SP, AP, AV, and AA (where S stands for scalar mesons, A stands for axial-vector mesons) modes are not considered in this paper since the decay constants and form factors for the scalar mesons f_0,, f_2 and the axial-vector meson a_1 are unknown to us. It is evident from Tables II–VII that the branching ratios of a large number of decay channels are in the range of a few times 10^{-5}, to be compared with the present experimental limit 10^{-4}. According to our calculation, decay modes such as $B_u^+ \to K^+\eta', \pi^+\eta', \rho^+\pi^0$, $\rho^+\eta', \rho^+\eta, \rho^+\omega$, $B_d^0 \to K^0\eta', \eta\eta', \eta'\eta', K^{+*}\pi^-, \rho^+\pi^-$, $K^{+*}\rho^-, \rho^+\rho^-$, should be accessible experimentally in the near future.

Since the decay modes $B_d^0 \to \pi^+\pi^-, \rho^+\pi^-, \rho^-\pi^+, \rho^+\rho^-$ are dominated by the external W emission diagram, the measurement of their branching ratios can be used to extract the KM mixing angle V_{ub}. Assuming $|V_{ub}/V_{cb}| \approx 0.1$, we find, for example, $B(B_d^0 \to \pi^+\pi^-) = 1.3\times 10^{-5}$, to be compared with the present limit 9×10^{-5} from CLEO and 13×10^{-5} from ARGUS.

It is worthwhile at this point to discuss and summarize the possible theoretical uncertainties one will encounter during the course of computation. The major sources of uncertainties are the following:

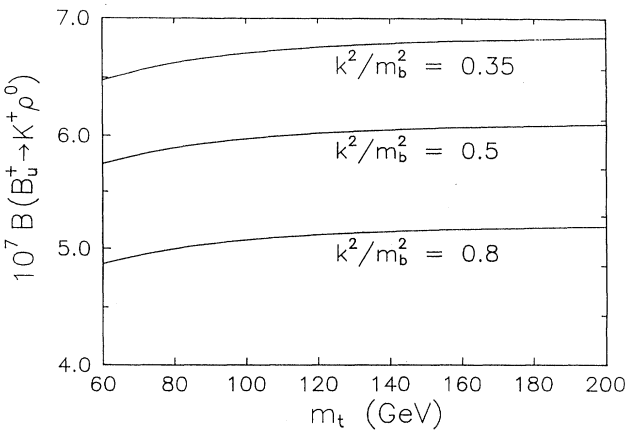

FIG. 2. Predicted branching ratios of $B_u^+ \to K^+\rho^0$ vs the top-quark mass for $k^2/m_b^2 = 0.8, 0.5, 0.35$.

(i) Form factors in various hadronic two-body matrix elements. There are basically two different approaches for form factors and they differ substantially for $B \to \pi, \rho$ transitions, see Sec. II B.

(ii) Annihilation and spacelike penguin diagrams. Since form factors at the momentum transfer $q^2 = m_B^2$ are unknown (except for the PP case), we do not know the size of annihilation and spacelike penguin contributions. Annihilation and spacelike penguin amplitudes in VP and VV modes are essentially neglected in our calculation. (It is however justified to neglect the spacelike penguin contribution in the VV case, as explained in Sec. IV D).

(iii) Final-state interactions. We have argued that final-state strong interactions are probably not important in charmless B decay since the two final-state light mesons are very energetic and hence do not have adequate time to allow significant strong interactions between them. However, we would like to study in the future the final-state interaction effects in a model-independent way in the dominant B decays as had been for charm decays.[14]

(iv) Renormalization-group effects on the penguin diagram. Thus far, leading-logarithmic QCD corrections have been considered only for inclusive penguin processes.[34]

(v) Unknown top-quark mass m_t and the virtual gluon momentum k^2. To study the k^2 and m_t dependence, we have calculated the decay rate of $B_u^+ \to K^+\rho^-$ as a function of m_t for three different values of k^2. As can be seen from Fig. 2, the predicted branching ratio is rather insensitive to the change of m_t, whereas it shows a significant k^2 dependence. It was argued in Ref. 35 that k^2 in exclusive two-body decays lies in the range $m_b^2/4 < k^2 < m_b^2/2$.

V. SUMMARY AND CONCLUSIONS

We have studied extensively the branching ratios of exclusive two-body decays of B_u^+ and B_d^0 without charm

particles in the final state. The salient feature of charmless B decay is that the W-loop diagrams play essential roles: either they predominate or their contributions are comparable to the spectator tree diagram in more than two-thirds of two-body rare B decay modes. Since the top-quark mass is greater than 77 GeV inferred from recent experiment, it is important to evaluate the W-loop penguin diagrams exactly for arbitrary m_t and virtual-gluon momentum k^2. As for the crucial mixing matrix element V_{ub}, its magnitude relative to V_{cb} was recently extracted from semileptonic decay by the ARGUS and CLEO Collaborations. Moreover, the phase of V_{ub} is fixed by the measurement of B_d^0-$\bar{B}_d^0$ mixing provided that the top quark is not too heavy.

In Sec. III we discuss the application of the quark diagram scheme, which eventually can provide a model-independent framework comparing with experimental results and checking the validity of calculations given in this paper, especially checking the assumption of the absence of final-state-interaction effects, and the validity of neglecting contributions from the W-exchange and W-annihilation diagram.

In Sec. IV we have calculated the decay rates for all rare decay modes $B \to PP, VP, VV$ using the factorization method. Possible theoretical uncertainties are discussed in Sec. IV D. We find that the branching ratios of a large number of decay modes are in the range of a few times of 10^{-5}. Especially, the following channels will have a good chance to be seen in the near future experimentally: $B_u^+ \to \pi^+\eta', K^+\eta, \rho^+\pi^0$, $\rho^+\eta', \rho^+\eta, \rho^+\omega$, and $B_d^0 \to K^0\eta', \eta\eta', \eta'\eta', K^{*+}\pi^-, \rho^+\pi^-, K^{*+}\rho^-, \rho^+\rho^-$.

In conclusion, the charmless rare B decays supply valuable opportunities to advance our understanding on dynamics of nonleptonic decays, especially the W-loop penguin mechanism.

ACKNOWLEDGMENTS

We would like to thank the CLEO group at Cornell for helpful discussions. We are grateful to Sheng-Nan Lai for drawing the figures in this paper. This work was supported in part by the U.S. Department of Energy, and the National Science Council of Taiwan.

APPENDIX A

Treating $c_2=(2c_+-c_-)/3$ as a free parameter in the vacuum-insertion method, we wish to determine the value of c_2 from the CLEO and ARGUS data[28] on the two-body decay modes $B_u^+ \to \psi K^+, \psi K^{*+}$, $B_d^0 \to \psi K^0, \psi K^{*0}$, and the inclusive decay $B \to \psi + X$. The experimental branching ratios for exclusive decays in units of 10^{-2} are

	CLEO	ARGUS
$B_u^+ \to \psi K^+$	$0.08\pm0.02\pm0.02$	$0.07\pm0.03\pm0.01$
$B_u^+ \to \psi K^{*+}$	$0.13\pm0.09\pm0.03$	$0.16\pm0.11\pm0.03$
$B_d^0 \to \psi K^0$	$0.06\pm0.03\pm0.02$	$0.04\pm0.03\pm0.01$
$B_d^0 \to \psi K^{*0}$	$0.11\pm0.05\pm0.03$	$0.11\pm0.05\pm0.02$

(A1)

Also,[36]

$$B(B \to \psi + X) = (1.12 \pm 0.20)\% \ . \tag{A2}$$

Following the calculation presented in Sec. IV C, we find

$$\Gamma(B_u^+ \to \psi K^+) = \Gamma(B_d^0 \to \psi K^0) = 2G_F^2 c_2^2 |V_{cs} V_{cb}^*|^2 |f_+^{BK}(m_\psi^2)|^2 \times m_\psi^2 f_\psi^2 m_B^2 p_{\text{c.m.}}^3 \ , \tag{A3}$$

where $p_{\text{c.m.}}$ is the center of momentum of the final-state particle. From the observed width of $\psi \to e^+e^-$, we obtain $f_\psi = 0.124$. Since $f_+^{BK}(0) = 0.379$ from Ref. 5, it follows that

$$B(B_u^+ \to \psi K^+) = B(B_d^0 \to \psi K^0) = 1.0 \times 10^{-2} c_2^2 \ . \tag{A4}$$

Comparing this with (A1), we get the averaged value $|c_2| \approx 0.26$.

The inclusive decay rate of $B \to \psi + X$ is estimated based on the assumption that $\Gamma(B \to \psi + X) \approx \Gamma(b \to \psi + s)$. Neglecting the small s-quark mass, we obtain

$$\Gamma(B \to \psi + X) \approx \frac{G_F^2}{16\pi m_b^3} c_2^2 |V_{cs} V_{cb}^*|^2 \times m_\psi^2 f_\psi^2 (m_b^2 + 2m_\psi^2)(m_b^2 - m_\psi^2)^2 \ . \tag{A5}$$

Comparison with the central value of (A2) yields $|c_2| \approx 0.27$. The calculation for $B \to \psi K^*$ is similar to that in Sec. IV B, and the final result is

$$B(B_u^+ \to \psi K^{*+}) = B(B_d^0 \to \psi K^{*0}) = 4.6 \times 10^{-2} c_2^2 \ . \tag{A6}$$

It is easily seen that $|c_2| \approx 0.17$, a value substantially smaller than the previous estimates. It seems to us that the discrepancy comes from the fact that the form factor for the B-K^* transition is somehow overestimated in Ref. 5. Indeed, the recent measurement of $D^+ \to \bar{K}^{*0} e^+ \nu$ by the E691 collaboration implies form factors for $D \to K^*$ smaller than the previous model predictions.[22] Hence, we take

$$\frac{2c_+ - c_-}{3} \simeq -0.25 \tag{A7}$$

to be the "experimental" value, where the sign is inferred from the $1/N_c$ approach and from the empirical fact that the interference of color-matched and color-suppressed amplitudes is destructive in the Cabibbo-allowed D^+ decays. Notice that for representative values $c_+ = 0.82$ and $c_- = 1.49$, $(2c_+ - c_-)/3$ is naively expected to be ≈ 0.05, whereas in the $1/N_c$ approach the QCD-corrected factor $(2c_+ - c_-)/3$ is replaced by $(c_+ - c_-)/2$ which is about -0.34.

APPENDIX B

The decay constants of the SU(3) singlet η_0 and SU(3) octet η_8 are defined by

$$\langle 0 | A_\mu^8 | \eta_8(q) \rangle = i f_{\eta_8} q_\mu \ , \qquad \langle 0 | A_\mu^0 | \eta_0(q) \rangle = i f_{\eta_0} q_\mu \ , \tag{B1}$$

where the axial-vector currents A_μ^8 and A_μ^0 are given by

$$A_\mu^8 = -\frac{1}{\sqrt{6}}(\bar{u}i\gamma_\mu\gamma_5 u + \bar{d}i\gamma_\mu\gamma_5 d - 2\bar{s}i\gamma_\mu\gamma_5 s) ,$$
$$A_\mu^0 = -\frac{1}{\sqrt{3}}(\bar{u}i\gamma_\mu\gamma_5 u + \bar{d}i\gamma_\mu\gamma_5 d + \bar{s}i\gamma_\mu\gamma_5 s) . \quad \text{(B2)}$$

Define the physical η and η' states by

$$\eta = \eta_8\cos\theta - \eta_0\sin\theta, \quad \eta' = \eta_8\sin\theta + \eta_0\cos\theta , \quad \text{(B3)}$$

with $\theta \approx -20°$. It follows from Eqs. (B1)–(B3) that

$$\langle 0|(\bar{u}u)|\eta\rangle = \langle 0|(\bar{d}d)|\eta\rangle = iq_\mu \frac{1}{\sqrt{6}}(\cos\theta f_{\eta_8} - \sqrt{2}\sin\theta f_{\eta_0}) ,$$
$$\langle 0|(\bar{s}s)|\eta\rangle = iq_\mu \frac{1}{\sqrt{3}}(-\sqrt{2}\cos\theta f_{\eta_8} - \sin\theta f_{\eta_0}) ,$$
$$\langle 0|(\bar{u}u)|\eta'\rangle = \langle 0|(\bar{d}d)|\eta'\rangle = iq_\mu \frac{1}{\sqrt{6}}(\sin\theta f_{\eta_8} + \sqrt{2}\cos\theta f_{\eta_0}) , \quad \text{(B4)}$$
$$\langle 0|(\bar{s}s)|\eta'\rangle = iq_\mu \frac{1}{\sqrt{3}}(-\sqrt{2}\sin\theta f_{\eta_8} + \cos\theta f_{\eta_0}) .$$

The ratio of f_{η_8}/f_π can be calculated in chiral perturbation theory with the result[37] 1.3 ± 0.05. As for the decay constant f_{η_0}, recent data on the two-photon width of η and η' yield[38] $f_{\eta_0} = (1.02\pm0.14)f_\pi$. Substituting f_{η_8} and f_{η_0} into Eq. (B4) gives

$$f_\eta^{(\bar{u}u)} = f_\eta^{(\bar{d}d)} \simeq 92 \text{ MeV}, \quad f_\eta^{(\bar{s}s)} \simeq -105 \text{ MeV} ,$$
$$f_{\eta'}^{(\bar{u}u)} = f_{\eta'}^{(\bar{d}d)} \simeq 49 \text{ MeV}, \quad f_{\eta'}^{(\bar{s}s)} \simeq 120 \text{ MeV} . \quad \text{(B5)}$$

We notice that when the mixing angle is $-19.5°$, the η and η' states become simply

$$|\eta\rangle = \frac{1}{\sqrt{3}}|\bar{u}u + \bar{d}d - \bar{s}s\rangle ,$$
$$|\eta'\rangle = \frac{1}{\sqrt{6}}|\bar{u}u + \bar{d}d + 2\bar{s}s\rangle . \quad \text{(B6)}$$

In SU(3) limit $f_{\eta_8} = f_{\eta_0} = f_\pi$, and hence

$$f_\eta^{(\bar{u}u)} = f_\eta^{(\bar{d}d)} = -f_\eta^{(\bar{s}s)} = f_\pi/\sqrt{3} = 77 \text{ MeV} ,$$
$$f_{\eta'}^{(\bar{u}u)} = f_{\eta'}^{(\bar{d}d)} = f_{\eta'}^{(\bar{s}s)}/2 = f_\pi/\sqrt{6} = 54 \text{ MeV} . \quad \text{(B7)}$$

Notice that the decay constant of η and η' given in Ref. 5 is evaluated under SU(3) symmetry and $\theta = -10°$.

*Present address: Physics Department, National Taiwan Normal University, Teipei, Taiwan 11718.

[1]L. L. Chau and H. Y. Cheng, Phys. Rev. Lett. **59**, 958 (1987).
[2]F. J. Gilman and M. B. Wise, Phys. Lett. **83B**, 83 (1979); for a review, see e.g., H. Y. Cheng, Int. J. Mod. Phys. A **4**, 495 (1989).
[3]S. Sharpe, in *Lattice '89,* Proceedings of the International Symposium, Capri, Italy, 1989 [Nucl. Phys. B (Proc. Suppl.) **17**, 146 (1990).
[4]M. Tanimoto, Phys. Lett. B **218**, 481 (1989).
[5]M. Bauer, B. Stech, and M. Wirbel, Z. Phys. C **34**, 103 (1987).
[6]N. G. Deshpande and J. Trampetic, Phys. Rev. D **41**, 895 (1990); D. S. Du, I. Dunietz, and D. D. Wu, *ibid.* **34**, 3414 (1986); Ya. I. Azimov, N. G. Uraltsev, and V. A. Khoze, Pis'ma Zh. Eksp. Teor. Fiz. **43**, 317 (1986) [JETP Lett. **43**, 409 (1986)]; M. B. Gavela *et al.*, Phys. Lett. **154B**, 425 (1985).
[7]F. Abe *et al.*, Phys. Rev. Lett. **64**, 142 (1990).
[8]H. Albrecht *et al.*, Phys. Lett. B **234**, 409 (1990).
[9]R. Fulton *et al.*, Phys. Rev. Lett. **64**, 16 (1990).
[10]M. Bander, D. Silverman, and A. Soni, Phys. Rev. Lett. **43**, 242 (1979).
[11]B. Guberina, R. Peccei, and R. Rückl, Phys. Lett. **90B**, 169 (1980).
[12]N. Deshpande and N. Nazerimonfared, Nucl. Phys. **B213**, 390 (1983); L. L. Chau, H. Y. Cheng, and W. Y. Keung, Phys. Rev. D **32**, 1837 (1985).
[13]The importance of the nonlogarithmic contribution 5/3 was stressed in H. Y. Cheng, Phys. Rev. D **37**, 1908 (1988); see also W. A. Bardeen, A. J. Buras, and J.-M. Gérard, Phys. Lett. B **180**, 133 (1986).
[14]See, e.g., L. L. Chau and H. Y. Cheng, Phys. Rev. D **36**, 137 (1987); Phys. Lett. B **222**, 285 (1989).
[15]A. J. Buras, J.-M. Gérard, and R. Rückl, Nucl. Phys. **B268**, 16 (1986).
[16]A. Soni (private communication).
[17]For a review, see M. Wirbel, in *Weak Interactions and Neutrinos,* Proceedings of the Twelfth International Workshop, Ginosar, Israel, 1989, edited by P. Singer and B. Gad Eilam [Nucl. Phys. B (Proc. Suppl.) **13**, 255 (1990)]; G. Kramer and W. F. Palmer, Phys. Rev. D **42**, 85 (1990).
[18]M. Wirbel, B. Stech, and M. Bauer, Z. Phys. C **29**, 637 (1985).
[19]B. Grinstein, M. B. Wise, and N. Isgur, Phys. Rev. Lett. **56**, 298 (1986); B. Grinstein, N. Isgur, D. Scora, and M. Wise, Phys. Rev. D **39**, 799 (1989).
[20]J. Bernabeu and C. Jarlskog, Z. Phys. C **8**, 233 (1981).
[21]A. Ali, J. G. Körner, G. Kramer, and J. Willrodt, Z. Phys. C **1**, 269 (1979).
[22]F. DeJongh, Ph.D. thesis, California Institute of Technology, 1990.
[23]L. L. Chau and W. Y. Keung, Phys. Rev. Lett. **53**, 1802 (1984).
[23(a)]Particle Data Group, J. J. Hernández *et al.*, Phys. Lett. B **239**, 1 (1990), p. III. 61.
[24]L. Wolfenstein, Phys. Rev. Lett. **51**, 1945 (1984).
[25]C. S. Kim, J. L. Rosner, and C. P. Yuan, Phys. Rev. D **42**, 96 (1990).
[26]F. J. Gilman and Y. Nir, Report No. SLAC-PUB-5198, 1990 (unpublished).
[27]L. L. Chau, Phys. Rep. **95**, 1 (1983); see also L. L. Chau, in *Proceedings of the Guangzhou Conference on Theoretical Particle Physics,* Guangzhou, China, 1980 (Van Nostrand Reinhold/Science, Beijing, 1980).
[28]D. L. Kreinick, in *Proceedings of the XIVth International Symposium on Lepton and Photon Interactions,* at Stanford, California, 1989, edited by M. Riordan (World Scientific, Singapore, 1989), p. 129; M. V. Danilov *ibid.*, p. 139; H. Albrecht *et al.*, Report No. DESY-90-046, 1990 (unpublished).
[29]The CLEO Collaboration, P. Avery *et al.*, Phys. Lett. B **223**,

470 (1989); D. Bortoletto *et al.*, Phys. Rev. Lett. **62**, 2436 (1989).

[30]The ARGUS Collaboration, H. Albrecht *et al.*, Phys. Lett. B **241**, 278 (1990).

[31]Of course, one may argue that helicity suppression could be alleviated by soft-gluon emission or by the existence of the soft-gluon component in the wave function of the heavy meson. Indeed, a critical analysis of data based on the quark-diagram scheme (Ref. 14) indicates that nonspectator contributions are not negligible in charm decay. In general, the helicity argument fails if the c.m. momentum of the final-state particle is comparable to the scale of the particle's mass, which is fortunaely not the case for charmless B decay.

[32]G. P. Lepage and S. J. Brodsky, Phys. Lett. **87B**, 359 (1979).

[33]J. G. Körner and G. R. Goldstein, Phys. Lett. **89B**, 105 (1979).

[34]R. Grigjanis, P. J. O'Donnell, M. Sutherland, and H. Navelet, Phys. Lett. B **213**, 355 (1988); **224**, 209 (1989).

[35]J.-M. Gérard and W. S. Hou, Phys. Rev. Lett. **62**, 855 (1989).

[36]See Table 3 of W. Maschmann *et al.*, Report No. SLAC-PUB-5133, 1989 (unpublished).

[37]J. Gasser and H. Leutwyler, Nucl. Phys. **B250**, 465 (1985).

[38]N. A. Roe *et al.*, Phys. Rev. D **41**, 17 (1990).